metals

MDPI

Review

Circular Recycling Strategies for LFP Batteries: A Review Focusing on Hydrometallurgy Sustainable Processing

David da Silva Vasconcelos *, Jorge Alberto Soares Tenório, Amilton Barbosa Botelho Junior and Denise Crocce Romano Espinosa

Department of Chemical Engineering, University of São Paulo, São Paulo 05508-080, Brazil
* Correspondence: david.vsc@usp.br; Tel.: +55-71-99188-1193

Abstract: The exponential growth of electric and hybrid vehicles in the last five years forecasts a waste problem when their batteries achieve end-of-life. Li-ion batteries for vehicles have been assembled using materials from natural resources (as Li, Fe, Al, Cu Co, Mn and P). Among them, $LiFePO_4$ cathode materials have demonstrated advantages such as charge–discharge cycles, thermal stability, surface area and raw materials availability (against Ni and Co systems). Due to the performance, LFP batteries stand out in heavy duty fleet, achieving 90% of new energy buses in China. To achieve the circular economy, the recycling of LFP batteries may be carried out by pyrometallurgy (thermal processing), hydrometallurgy (aqueous processing) or both in combination. Comparatively, hydrometallurgical processing is more advantageous due to its low energy consumption and CO_2 emissions. In addition, Li may be recovered in a high-pure grade. This work is a literature review of the current alternatives for the recycling of LFP batteries by hydrometallurgy, comparing designed processes in the literature and indicating solutions towards a circular economy. The major recycling steps of hydrometallurgy routes such as pre-treatments, leaching and purification steps will be gathered and discussed in terms of efficiency and environmental impact.

Keywords: electric vehicle; lithium iron phosphate; acid leaching; precipitation; solvent extraction; ionic exchange; ionic liquids; deep eutectic solvents

Citation: Vasconcelos, D.d.S.; Tenório, J.A.S.; Botelho Junior, A.B.; Espinosa, D.C.R. Circular Recycling Strategies for LFP Batteries: A Review Focusing on Hydrometallurgy Sustainable Processing. *Metals* **2023**, *13*, 543. https://doi.org/10.3390/met13030543

Academic Editor: Jean François Blais

Received: 6 February 2023
Revised: 27 February 2023
Accepted: 3 March 2023
Published: 8 March 2023

1. Introduction

Lithium-ion batteries (LIBs) have been gradually replacing other batteries such as lead-acid, nickel–metal hydride and nickel–cadmium storage technologies due to their higher energy density, life cycle and low self-discharge [1,2]. LIBs have a feasible specific energy density between 100 Ah/kg and 165 Ah/kg, allowing for applications in compact devices and electric vehicles. Additionally, their inherently higher life cycle (500 to 2000 charge and discharge cycles) and their cost decreasing from USD 1100/kWh in 2011 to USD 150/kWh in 2022 enhanced their attractiveness [3].

LIBs are used in different applications: electric and electronic equipment (EEE), energy storage systems (ESS) and electric vehicles (EV). EEEs include laptops, smartphones, tablets, e-scooters, e-bikes and small household devices. Once applied for industrial purposes or for energy storage from renewable sources (for instance, wind and solar), LIBs are classified as ESS. Other applications include vehicles, such as pure electric vehicles (EV), plug-in hybrids (PHEV), hybrid electric vehicles (HEV) and motorized two-wheelers [4].

Currently, LIBs are the most common technology applied to EVs and account for more than 40% of EVs' prices. An on-board LIB pack in an EV contains hundreds of single-LIB cells packed together to provide a combined power supply, with the absence of tailpipe emissions and a reduced carbon footprint [5]. For example, the Nissan Leaf 24 kWh battery pack has 192 cells and weighs 290 kg, and the Chevrolet Volt 16 kWh battery pack has 288 cells and weighs 197 kg [6].

Among LIBs, LFP batteries take advantage of the absence of Co and the phosphate's capacity to stabilize the structure, enhance the electrode stability against overcharging and provide a higher tolerance to heat [7]. In this sense, an LFP cathode tends to dominate large-sized applications such as buses, large vehicles and large equipment [8]. In the future, the recycling of spent LFP batteries from EVs will be a secondary source of critical raw materials (Li, P and C) [9].

Thus, the main objective of this review is contemplating the recycling paths of LFP batteries, in terms of circular economy. The hydrometallurgical process will be discussed because of its environmental compatibility, lower energy demand, high-priced products and less air pollution. Leaching and purification steps will be gathered and discussed in terms of efficiency and environment protection.

2. Lithium-Ion Batteries (LIBs)

Figure 1 depicts the battery cycles and set-up configuration of inner components. The main components in commercial LIBs cells are the positive and negative electrodes (cathode and anode), separator and electrolyte, all of them involving a metallic extern protection. The cathode has an active material bonded in an aluminum foil, and each active material in the cathode generates a different type of battery (Section 2.1). The anode usually has graphite bonded in a copper foil.

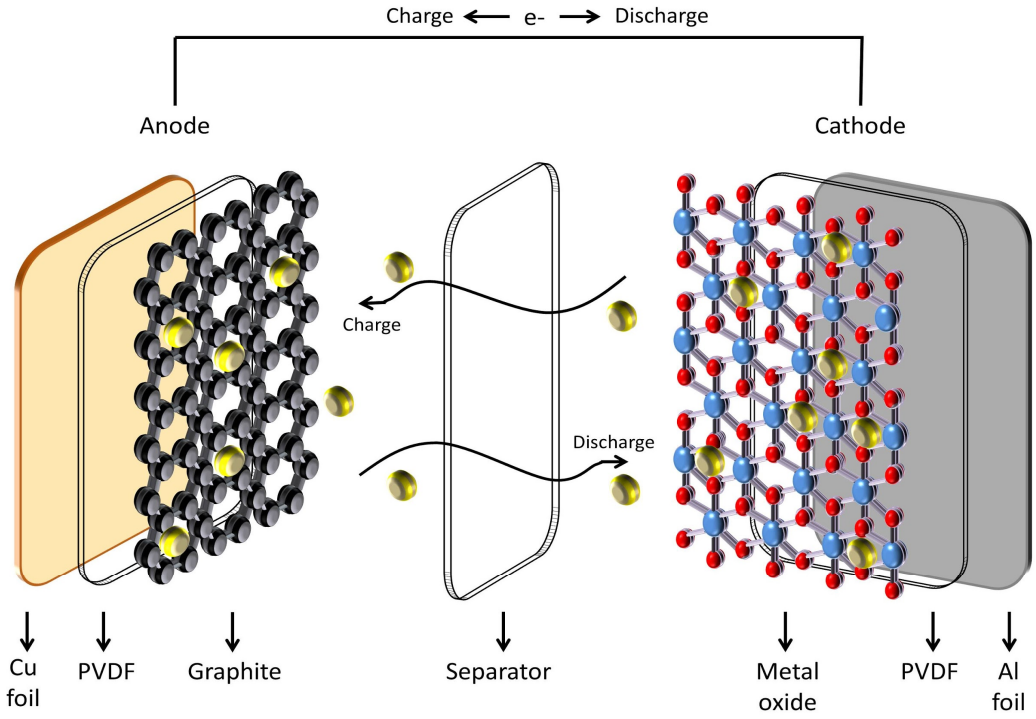

Figure 1. Charge and discharge process in LIBs. Ionic transfer between the cathode and anode [10].

Ref. [11] summarized the mass percentages of each component for three common batteries on the market. Metallic extern protection or housing may be of metallic aluminum or steel and vary between 17 and 27% of the mass percentage of the cell. The cathode has two main components, active material and aluminum foil, varying between 26% and 41% for the active material and 4 and 7% for the aluminum foil. In the anode, the main components are the anode active material and copper foil, corresponding to 13–18% and 7–17% of the cell, respectively. The separator corresponds to 3% of the cell, and the electrolyte varies between 10 and 16%. As reported by the authors, the mass fraction of each component in battery cells must change among different manufacturers.

2.1. Cathode Materials

The cathode is a composite material with active material coated in an aluminum foil. Polyvinylidene fluoride (PVDF) is usually used to bond the active material at the Al foil [12]. It might have conductive carbon and additives for improved performance [13].

The active material is a black powder constituted by oxides of transition metals (TMO_2); the composition determines the type of battery. Commercial LIBs have been developed with the chemical formulas $LiNi_xMn_yCo_zO_2$ (NMC), $LiNiO_2$ (LNO), $LiMn_2O_4$ (LMO), $LiNi_xCo_yAl_{1-x-y}O_2$ (NCA) and $LiCoO_2$ (LCO). There is also the active material composed of phosphate of lithium and iron—$LiFePO_4$ (LFP). Crystalline structures reported in commercial LIBs are layered (LCO, NCA and NMC), spinel (LMO) and olivine (LFP).

The chemical composition and crystalline structure must change the electrical properties. Also known as intercalation materials (IMs), those oxides should accept or release Li+ at the crystalline structure with the generic redox reaction described in Equation (1).

$$TMO_2 + xLi^+ + xe^- \leftrightarrow Li_xTMO_2 \quad (1)$$

Li incorporation into oxides' crystalline structure must occur with low-volume expansion and contraction to provide mechanical and electrochemical stability and long-term use for the battery [14]. Other characteristics of intercalation materials include the weak structure perturbation by the incorporation of metal-ions, the low concentration of transition metal ions in the structure and the host stoichiometries for Li^+ 1:1 or 1:2 [14].

In a layered structure model, two octahedron units (LiO_6 and TMO_6) should be selected, and Li diffusion throughout the oxide is directly influenced by the valence state of TM ions and the size of TMO_6 [15]. In general, high nickel contents in transition metal oxides lead to a higher specific capacity of 270–285 Ah/kg for NMC batteries [16].

Lithium manganese oxides ($LiMnO_2$ or $LiMn_2O_4$) should have several compositions, but the $LiMn_2O_4$ spinel is the most applied in commercial LIBs. In spinel crystalline structures, octahedral and tetrahedral structures intercalate in the spatial arrangement. This cathode stands out for a three-dimensional diffusion pathway, which guarantees good reversibility for charging and discharging, despite the lower specific capacity of 110 Ah/kg compared to that of other cathode materials in Table 1.

Table 1. Comparison among cathode materials [16].

Cathode	$LiCoO_2$	$LiMn_2O_4$	$LiN_xM_yC_zO_2$	$LiFePO_4$
Tap density (kg/m^3)	2.8–3.0	2.2–2.4	2.0–2.3	1.0–1.4
Specific surface area (m^2/kg)	400–600	400–800	200–400	1200–2000
Theoretical specific capacity (Ah/kg)	274	148	270–285	170
Specific capacity (Ah/kg)	135–140	100–115	155–165	130–140
Voltage (V)	3.6	3.7	3.5	3.2
Cycle life	300 cycles	500 cycles	800 cycles	2000 cycles
Abundance of raw materials	Poor	Abundant	Poor	Very abundant
Cost of raw material	Very expensive	Cheap	Expensive	Cheap
Environment	Containing cobalt	Nontoxic	Containing nickel and cobalt	Nontoxic
Safety	Poor	Better	Better	Best

Iron phosphate batteries ($LiFePO_4$) have the same structure as olivine minerals. In this crystalline network, FeO_6 disposes in octahedrons, forming plane structures connected by PO_4 tetrahedra. These FeO_6 octahedra structures share oxygen bonds with LiO_6 octahedrons, forming a 1D channel for Li-ion diffusion [15]. This molecule stands out in the

absence of nickel and cobalt and may achieve a 170 Ah/kg theoretical specific capacity and a 3.5 V cell voltage against the graphite anode [7].

Table 1 summarizes comparative analyses among commercial LIBs. The LFP cathode has the best safety in comparison with other cathode materials because of the phosphate's capacity to stabilize the structure, enhance electrode stability against overcharging and provide a higher tolerance to heat, which limits the thermal runaway [7].

Despite the advantages of the LFP cathode performance, its chemistry has shown drawbacks in EVs. The olivine structure has a lower theoretical specific capacity than NCA ($LiNiCoAlO_2$) and NMC ($LiN_xM_yC_zO_2$) chemistries and a limited nominal potential in 3.2 V, causing LIBs manufacturers to choose high potential cathodes for power gain with a smaller battery package [17]. Furthermore, Li ions diffusion hardly affects LFP batteries' efficiency once it has poor electrical conductivity (10^{-9} to 10^{-8} S/cm), ionic conductivity (10^{-11} to 10^{-9} S/cm) and ionic diffusivity (10^{-17} to 10^{-12} cm^2/s) [18]. Additionally, LFP batteries have a low electrochemical performance at temperatures below 0°C [19]. These drawbacks lead to a difficult application for high-capacity EVs, and efforts have been made to enhance their efficiency.

For this reason, the LFP cathode has characteristics that lead to a share of the world market of 2% in 2020 [20]. Improvements in Li ion diffusion and electrical conductivity have led to the LFP cathode dominating electric bikes and heavy-duty fleet [8]. The high cycle performance (2000 cycles), thermal stability, low density (1.0–1.4 kg/m^3) and high surface area (1200–2000 m^2/kg) stimulated the large-sized applications, including in large equipment. Due to the performance, about 90% of new energy buses in China are equipped with LFP batteries [16]. Therefore, LFP batteries have an important share in the large vehicle market.

2.2. $LiFePO_4$ Cathode

The safety of LFP batteries is due to $LiFePO_4$ two-phase lithiation, leading to a stable voltage plateau in contrast to the single-phase intercalation process of layered oxide materials [21]. Equation (2) summarizes electrochemical reactions at the electrode/electrolyte interface; the direct reaction of equilibrium consists in the discharge process. Separating by electrodes, Equation (3) indicates the lithiating process in the cathode. Equation (4) shows the reactions in the anode.

$$Li_nC_6 + Li_{m-n}FePO_4 \leftrightarrows Li_0C_6 + Li_mFePO_4 \quad (2)$$

$$Li_{m-n}FePO_4 + nLi^+ + ne^- \leftrightarrows Li_mFePO_4 \quad (3)$$

$$Li_nC_6 \leftrightarrows Li_0C_6 + nLi^+ + ne^- \quad (4)$$

Once the LFP crystalline structure has only one diffusion path for Li-ions, the good cathode performance depends on synthesis parameters. An adequate cathode preparation must avoid impurities, reduce the active material cost and improve electrochemical characteristics.

The cathode active material ($LiFePO_4$) may be produced by a solid-state reaction, mixing Fe and Li sources ($FePO_4$ and $LiCO_3$) under an inert atmosphere and high temperatures. Frequently, this process led to few impurities in the final product, such as $Li_3Fe_2(PO_4)_3$, Fe_2O_3 and $LiPO_4$ as subproducts of the thermal treatment [13]. To obtain fine particles, avoid impurities and improve electrochemical properties, wet-synthesis routes such as precipitation, sol–gel, polyol, hydrothermal, solvothermal, reverse micelle and spray pyrolysis have been explored [13–22].

The carbon coating process has been widely applied because the conductive carbon layer increases the electron migration rate during the charge/discharge cycles [23]. Carbon coating is commonly obtained in the synthesis of LFP cathodes at solution routes, dispersing carbonaceous materials in an aqueous or nonaqueous solution. The product of this process is an $LiFePO_4$/carbon composite. The surface covered with conductive carbon also contributes to reducing the particle size, inhibiting particle growth during sintering [19]. The size of the particles decreased as the carbon content increased. Finally,

LFP/C composites with about 2 wt% carbon covering displayed an improved discharge capacity, capacity retention and rate capability compared to those without coating [22].

2.3. Anode Materials

The most common anode active material of the commercial LIBs is carbon-based (graphite), while other materials such as graphene and lithium titanate ($Li_4Ti_5O_{12}$) are possible. Graphite has a high specific capacity of 370 Ah/kg and a low average voltage (150 mV vs. Li/Li^+) [7]. Graphite stands out in LIBs applications due to its high electrical conductivity, low cost, mature production process and abundant resources [24].

Graphene has a specific capacity of 744 Ah/kg because both sides of the graphene may host Li ions (Li_2C_6) [24]. This guarantees that graphene has a two times higher specific capacity than graphite anode. Lithium titanate (LTO) is based on a redox couple (Ti^{4+}/Ti^{3+}), which works at approximately 1.55 V and has a specific capacity of 175 Ah/kg [25].

2.4. Separator

The separator is a physical porous membrane soaked in electrolytes that leads Li-ions to move between the cathode and anode. As one of the key components for LIBs, the separator avoids short-circuiting during the battery operation, promotes lithium ions transfer between the electrodes, regulates cell kinetics and suppresses the formation of dendrite structures [26]. There are four types of battery separators: single/monolayer polymers, polymer blends, composites and solid separators.

Single polymers are separators based on a monolayer of polyolefins such as polyethylene (PE) and polypropylene (PP). The fabrication process aims to control key parameters such as pore diameter and porosity while soaked with the electrolyte. Low-porosity and small-pore-sized membranes protect the internal short circuit, while high-pore-sized membranes enhance ion conductivity [27]. Those polymers are widely used in commercial LIBs due to their affinity with electrolytes, mechanical strength, short migration paths for Li-ions, electrochemical stability and cost-effectiveness [28]. Furthermore, PE separators are preferred, as they show an improved cyclic stability in comparison with PP separators [29].

Polymer blends are usually the combination of PE and PP, forming bilayer PE/PP or multilayer PP/PE/PP. Those separators are commonly called “shutdown separators”, owing to the fact that they act as a safety device, based on the lower melting point of PE compared to that of PP. Once the internal temperature rises to the melting point of PE, it melts to close the inner pores of the PP structure, preventing Li-ions diffusion and stopping electrochemical reactions [30]. Blends of polymers would raise the melting point of the mixture, enhancing thermal stability and sustaining the ionic diffusion throughout the membrane [31].

New batteries have tested composite membranes to enhance thermal stability, overcoming the low melting point of polyolefin-based separators. Ceramic-coated separators (CCS) stand out with the commercial application because of the enhanced physical properties, thermal stability and cost-effectiveness [32].

The CCS is a composite membrane formed by a polyolefin separator (PE and PP), with ceramic materials coated on the surface (Al_2O_3, MgO, SiO_2 and γ-$LiAlO_2$) [27]. Polymeric binders such as polyvinylidene fluoride-hexafluoropropylene (PVDF-HFP), polymethyl methacrylate (PMMA) and polyvinylidene fluoride (PVDF) have been used for coating inorganic material onto the polyolefin membrane [33]. Despite previous advantages, there is still a safety issue due to the low melting point of the binders, which should desquamate the ceramic layer and raise the total cost of the separator [33].

2.5. Electrolyte

Liquid electrolytes are the standard physical media for ion conduction in most commercial electrochemical energy storage devices, including LIBs [34]. Conventional LIBs electrolytes are composed of carbonate liquid solvents, either singular or a mixture of them, with lithium salt and organic additives dissolved into those solvents [35]. In gen-

eral, the electrolyte is mixed with about 12 wt% lithium salt, 83 wt% solvent and 5 wt% additives [36].

Organic solvents make up a higher proportion in the electrolyte mixture and must exhibit a high dielectric constant (ε_0), low viscosity (η), a high flash point, nontoxicity and economic feasibility. Further, the solvent maintains the chemical stability of the cells and must remain at the liquid state during the battery operation (wide temperature range between the melting and boiling point) [37]. The term "green solvents" has specified organic solvents that show characteristics such as a low toxicity, low vapor pressure and biodegradability [38].

LIBs have used nonaqueous solvents, commonly aprotic apolar, due to Li electrolytes' reactivity in water [21]. The use of green solvents has been increasing, such as organic carbonates, which present a large liquid temperature range (melting point = −49 °C and boiling point = 243 °C), low toxicity and biodegradability [38]. Further, organic carbonates have a large supply chain for attaining a high LIBs demand [39].

The literature has reported the use of organic solvents such as ethyl carbonate (EC), propylene carbonate (PC), methyl ethyl carbonate (EMC), dimethyl carbonate (DMC) and diethyl carbonate (DEC). Linear carbonates present a high dielectric constant, leading to high ionic conductivity and good penetrating ability into polyolefin-based separators, decreasing the electrolyte viscosity and forming a stable solid electrolyte interface (SEI) film on the graphite surface electrode [40].

The cathode's contact with the electrolyte at high voltages causes the oxidation of solvent molecules, while the anode depends on the formation of an SEI. Further, the graphite structure can be easily destroyed during the intercalation/deintercalation of lithium ions and electrolytes into the graphite layer at a high C-rate or after long-term cycling [41]. In order to improve the solvent ionic conductivity and effectively passivate electrodes, lithium salts such as $LiPF_6$, $LiPF_4$, $LiAsF_6$, $LiClO_4$, $LiCF_3SO_3$ and $LiBC_4O_8$/LiBOB have been used [36]. Among them, lithium hexafluorophosphate ($LiPF_6$) is the main salt in commercial LIBs [2].

The solid electrode interface (SEI) is a thin layer formed on the anode surface, composed of Li_2O, LiOH, $(LiCO_2)_2$, $LiOCH_3$, Li_2CO_3 and LiF (being the main reagent) [41]. A desirable SEI film should be electron-insulating, uniformly and compactly cover the graphite surface and allow for Li+ diffusion paths at the anode [42]. Throughout this solid interface, lithium ions transfer from lithiated graphite (LiC_6) to the solution, or the opposite path. One of the SEI possibilities, for instance, is the layer of LiF at the graphite edge produced by the decomposition of $LiPF_6$, as depicted in Equation (5) [41].

$$LiPF_6 \rightarrow LiF + PF_5 \quad (5)$$

Electrolytes such as $LiClO_4$, $LiBF_4$ and $LiPF_6$ have high toxicity. The standard electrolyte in commercial LIBs ($LiPF_6$) showed a high reactivity upon the exposure to air and might hydrolyze. In contact with air moisture by incorrect disposal in soils, this salt releases HF, causing serious environmental damages (Figure 2). Equations (6) and (7) present the decomposition of $LiPF_6$ that might occur, even at room temperature [37]. Initially, PF_5 is formed by the reaction with water traces, which should produce hydrofluoric acid (HF), lithium fluoride (LiF) and phosphoric acid (H_3PO_4) [21–43].

$$LiPF_{6(sol.)} + H_2O \leftrightarrow LiF_{(s)} + 2HF_{(sol.)} + POF_{3(sol.)} \quad (6)$$

$$PF_{5(sol.)} + H_2O \leftrightarrow 2HF_{(sol.)} + POF_{3(sol.)} \quad (7)$$

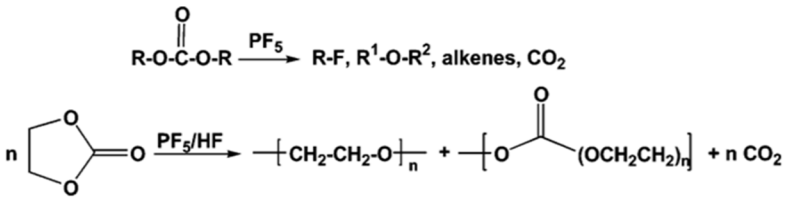

Figure 2. Carbonates decomposition by PF_5 [37].

3. LIBs Demand and Waste Generation

Recently, the mature stage of LIBs technology has led to a rapid increase in its application for electric vehicle (EV), plug-in hybrid electric vehicles (PHEV) and hybrid electric vehicles (HEV). EVs have only electric batteries as the power supply. The difference between PHEV and HEV is the higher battery size in PHEV, which allows for running long distances with only electric power [44].

Figure 3 depicts the global electric vehicles on the road from 2010 to 2021 [45]. In 2014, 1 million EVs were on world's roads, and electrification became more evident in the following years. Between 2019 and 2020, the world's EVs fleet increased by 43%, with the number of EVs being higher than 10 million [46]. In 2021, 16.5 million EVs were on the roads, and sales achieved 9% of the global car market share [45].

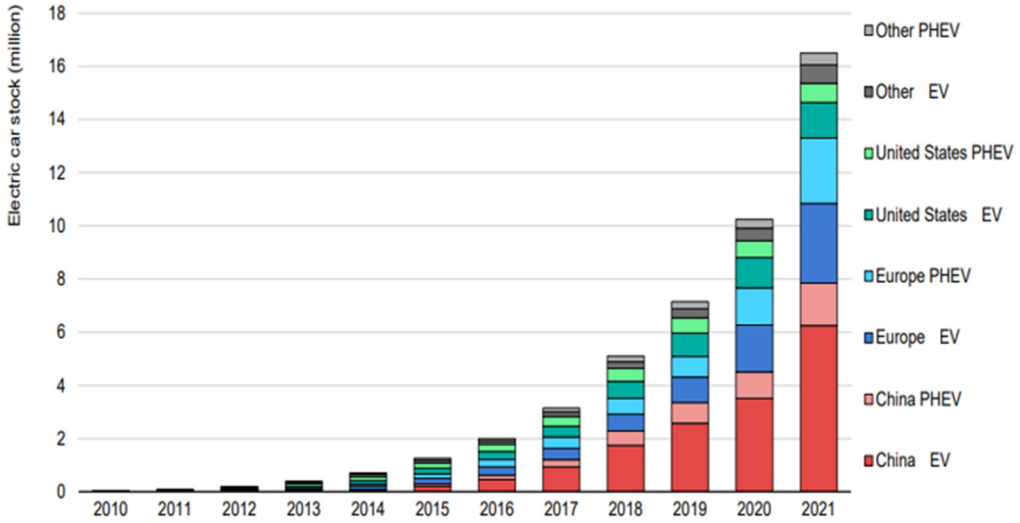

Figure 3. Electric cars on the world's roads in 2021 [45].

China maintained the world's largest EV fleet in 2021 with 7.8 million units, followed by the European Union, with 5.5 million, and the USA, with over 2 million in 2021 [45]. China is expanding its market, having employed government subsidies for EVs during pandemic (2020–2022), and the country achieved the mark of 16% electric cars sales in the domestic market [45]. The European Union achieved the mark of 17% of EVs in auto sales, and the USA achieved a market share of 4.5% of EVs. Compared with 2020, the market share of EVs in auto sales was 5.7%, 10% and 2% in China, the EU and the USA, respectively [46]. The EV market will have a strong influence in the EU, the USA and the BRICS countries [10].

Countries such as the Netherlands, Norway, France, India and the United Kingdom have explicitly launched a ban on selling internal combustion vehicles in the coming years [47]. The Norwegian Parliament has decided that all new passenger cars and light vans should be zero-emission by 2025. The country has been stimulating the EVs market through the exemption of registration taxes for new EVs, free access to bus lanes, reduced parking fees and rebates in car ferry crossings [48].

The increased demand for LIBs tends to generate high amounts of spent LIBs waste during manufacturing and end-of-life (EoL). When LIBs achieve an 80% rate capacity, they no longer meet the requirements for EVs applications. After that, the batteries should be applied in less-demanding capacity applications and then enter the end of life with less than 60% initial capacity, becoming electronic waste [49]. It is predicted that more than 25 billion units and 500 thousand tons of LIBs will become waste in 2020 [50].

China has been the largest electric vehicle market and battery manufacturer since 2019 [51]. With the exponential growth of the EVs market in China, many LIBs will be scrapped soon, making it the country with the most spent LIBs generated [36]. It is estimated that the total number of spent batteries in China will reach 605,800 tons in 2030, while about 313,300 tons will be from spent $LiFePO_4$ batteries [52].

4. Critical Raw Materials

As shown in previous sections, companies have assembled LIBs with several compositions. The demand and pression for the electrification of the vehicles fleet has created a scenario of increasing the production of raw material and mineral extraction to supply the LIBs market. $LiFePO_4$ batteries materials that are receive special attention are Li, graphite and phosphate minerals. Those materials are classified as critical for a wide group of countries, while other metals such as Cu, Al and Fe have abundant resources [10].

Natural graphite is an abundant material on earth, but only China has 70% of the world's production share in 2017 [53]. The supply concentration in some countries has led the market to mix synthetic and natural graphite for LIBs applications, despite synthetic graphite's cost (almost double that of natural graphite) [54]. Further, the major part is destined to steelmaking, impacting the availability of natural graphite for battery applications. By 2050, the global graphite demand for energy storage applications is expected to increase by 500% compared with that in 2018 [55].

Mined phosphorous is majorly destined to the food industry, with 85% of the global production destined to fertilizers and 10% to animal feed supplements [56]. In estimating the demand of phosphorous per year, considering the increase in the EVs and LFP markets, around 5% of the current global phosphorous demand will be just from light electric vehicles by 2050 [56], drawing attention to the competition between the food and energy industries. On the other hand, in the largest LFP batteries market (China), 102.90 million tons of phosphate rocks (30% of P_2O_5) were produced in 2022, increasing by 13.8% compared to the previous year [57].

Chile and Argentina are the major producers of Li from brines, while Australia and China stand out in mines extraction [58]. The global consumption of lithium in 2020 was estimated to be 70,000 tons, and it was 93,000 tons in 2021 (which represents a 33% increase) [59]. The increase in global Li consumption may be related to the end-use of Li in batteries. The final destination of Li to batteries has changed from 34% in 2015 to 74% in 2022, pushed by the demand for EVs and portable electronic LIBs [59,60]. Only China accounts for 50% of the Li global consumption, and it is the world's largest consumer [36]. The cumulative demand for Li in China will exceed the current Li reserves by 2028 [61].

Commodity production should be affected for political and social issues. The biggest world suppliers may protect their domestic market, restricting imports and causing market stress and uncontrolled prices. Further, increasing demand in the sector of renewable energy raised prices for the abovementioned raw materials. Concerns about the supply chain of raw materials for LIBs production led countries to classify some commodities as critical or strategic raw materials [59–62].

According to the European Union (EU), critical raw materials include materials with economic importance and supply risks for the bloc. The EU list of 2020 contains 30 materials, including materials important for cathode and anode manufacturing. Materials such as cobalt, phosphate rock, phosphorous, natural graphite and bauxite (aluminum source) have been listed since 2017, while Li was included in 2020. The increasing demand for graphite and phosphorous, along with the import dependence of the EU, includes those

minerals as critical for the bloc. Despite the absence of iron in the list of critical materials, EU countries do not have iron natural resources, except for Sweden, with a production of 35 million metric tons per year, representing 1.5% of the global iron ore production in 2020 [63].

The USA geological survey disposed a list of "salient critical mineral statistics". Critical minerals are defined as minerals that are essential for economic or national security, are under supply chain interruption risks or serve to manufacture an essential product [59]. The USA is totally dependent on the import of its critical list once the consumption surpasses the primary and secondary productions. The list includes cobalt, manganese, lithium, natural graphite and aluminum (the latter being included in the fabrication of LFP batteries as an electron collector and cases). Bauxite (Al) stands out with the highest consumption among the listed materials, but Li and natural graphite have more scarcity and impact the applications for renewable storage systems [64].

Brazil summarizes the "strategic materials", which are raw materials that are heavily dependent on imports or minerals of which the country has an abundance in natural reserves and production [10]. The materials listed as strategic for Brazil, regarding LIBs applications, include: lithium, aluminum, copper, cobalt, iron, manganese and phosphor [65]. Brazil still needs more studies summarizing the critical raw material for the national economy and evaluating the domestic and importations supply risk [66].

Those materials do not have primary or secondary production (lower than 5%, in spite of the fact that 95% of aluminum cans, for instance, are recycled), indicating that the recycling process should be an alternative to promote the circular economy and the reinsertion of materials into the production chain. For instance, the lithium secondary production recovered from end-of-life LIBs must significantly reduce the need for lithium raw materials [36].

5. LIBs Waste and Circular Economy

The extensive use of LIBs must raise the number of spent LIBs generated every year. In those spent LIBs, there are many valuable chemicals (Li, P, C, Ni and Co). Furthermore, incorrect disposal would be harmful for the environment. Some components such as organic flammable solvents and toxic salts classified spent LIBs as hazardous waste [67]. Spent LIBs must be disposed safely and properly recycled to avoid polluting the environment and recovering the valuable metals [68].

The circular economy is a concept designed to change the linear chain of the products life cycle (take–make–use–dispose) to a model that reintroduces residues in the market. For this model, all material and energy streams need to be reintroduced to the economy cycle [69]. In an ideal scenario, all of the energy input into the cycle comes from renewable resources, and the input of virgin raw material might be reduced [70]. Reducing, reusing, refurbishing and recycling are the major ways to reintroduce material raw materials to the life cycle chain.

Reducing has an intrinsic relation with the fabrication of new LIBs. The manufacture of new LIBs should consider second uses and recycling, as well as the substitution of critical raw materials in LIBs. The cobalt content has been reduced in cathode active material, replacing it with a high Ni content (NCA and NMC) or substituting it for other battery types, such as LFP batteries (without Co and Ni). In addition, the substitution for Fe phosphate is benefited due to its abundant sources and reducing Co extraction from D.R. Congo (the main Co resource in the world, related to social and political issues) [54].

Reusing spent LIBs is to give them a second life. Spent LIBs from EV applications that retain 80–85% of their original capacity may be directly applied in stationary uses [71]. Less essential purposes such as residential backup systems and generating energy for LED (light emitter diode) would not demand a high energy density and must consist of reusing spent LIBs from EVs applications [1]. In recent years, second utilization has attracted wide attention because it extends the LIBs life cycle, reduces the cost of batteries for EVs and

other applications, alleviates the recycling pressure, reduces the raw material demand and promotes a circular economy for LIBs [69].

Refurbishing is sometimes needed for secondary applications. Refurbishing at the cell level consists of disassembling batteries modules into single cells; then, the cells are tested and sorted to be remanufactured into a new module for lower-energy-density applications [69].

Recycling is a fundamental path to achieving an LIBs circular economy. Reducing, reusing and refurbishing should postpone the LIBs life cycle but will not recover the components of the spent cells. Recycling might be a way to recover valuable chemicals, save natural resources and avoid the environmental impact hazards involved in mining activity, the manufacture of new LIBs and incorrect disposal [72].

Recyclers are interested in NMC batteries due to the intrinsic value of Ni and Co. Despite this, a heavy duty fleet has the potential to produce high amounts of battery waste, and the volume of LFP batteries disposed must not be neglected. Once LFP batteries are classified as hazardous waste, the final users may pay for the final disposal, increasing the attractiveness of recycling LFP batteries.

6. Recycling Routes

6.1. Industrial Processing

LIBs may be recycled by pyrometallurgy, hydrometallurgy or combination of both [73]. Figure 4 depicts the steps for LIBs recycling. Batteries recycling starts with discharging to avoid short circuits; then, the cells may be dismantled or directly comminuted (pre-treatment steps). Metal extraction is the pyro/hydrometallurgical step, which involves the recovery of metal using temperature or acid solutions. Then, the metal may be separated in the purification steps.

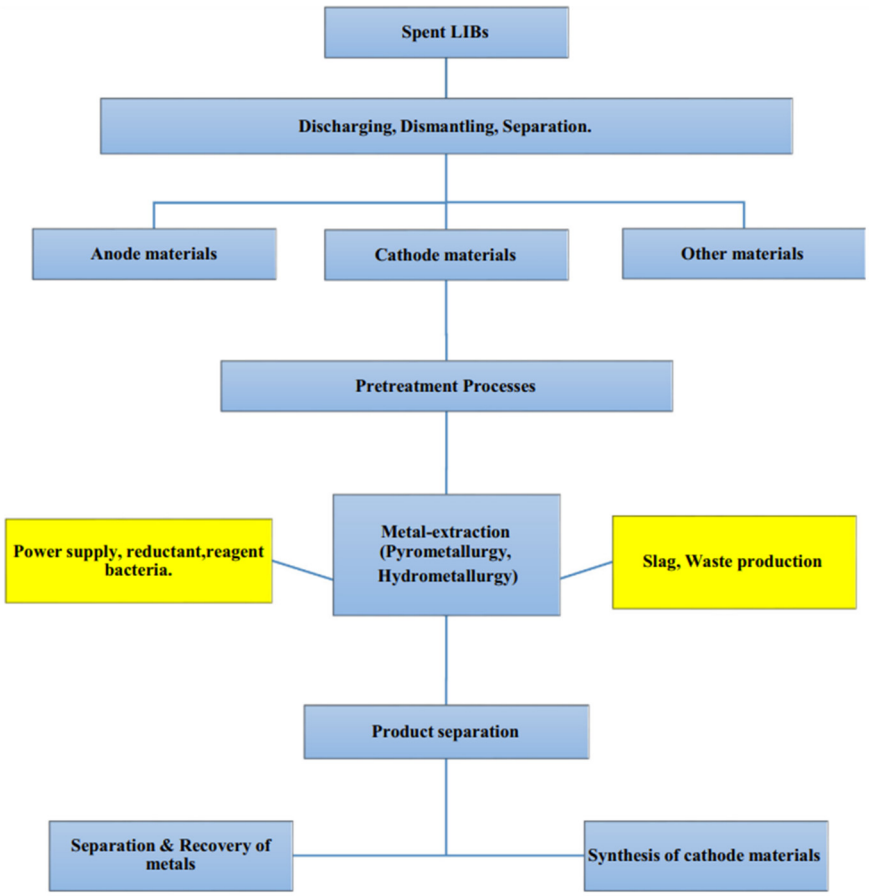

Figure 4. Classical recycling process for spent lithium-ion batteries [9].

Table 2 summarizes the recycling process of the main recycling companies. Pyrometallurgy is the most common method currently used, such as by Umicore (Belgium), Inmetco (USA) and JX Nippon (Japan) [74,75]. Hydrometallurgy remains a part of a few industrial applications in battery recycling, the most important being Retriev (Canada and US) and Recupyl (France) [76].

Table 2. Current major commercial processes for recycling spent LIBs [10,74–76].

Company	Country	Capacity (ton/year)	Recycling Process	Products
Umicore	Belgium	7000	Pyro-dominant	Ni-Co alloy, $NiCO_3$, $NiSO_4$, $CoCO_3$, $CoSO_4$
Xstrata (Glencore)	Switzerland	7000	Pyro-dominant	Co alloy
Inmetco	USA	6000	Pyro-dominant	Co–Ni–Fe alloy
Accurec	Germany	6000	Pyro-dominant	Li_2CO_3
JX Nippon Mining and Metals	Japan	5000	Pyro-dominant	Co Alloy
Retriev	Canada	4500	Hydro-dominant	Li_2CO_3 and Ni
Recupyl	France	110	Hydro-dominant	$MnCO_3$ and Co

Among industrial plants (Table 2), Accurec recovers lithium by combining pyrolytic and hydrometallurgical process steps. The final products are lithium carbonate (Li_2CO_3) and high-priced metal alloys [60]. Further, lithium recycling processes are carried out by AEA Technology Group plc (UK), by Batrec Industrie AG (Switzerland) as well as by Recupyl (France) [60].

$LiFePO_4$ batteries are forecasted to become a waste problem in the future, as China represents a large consumer for the application of large vehicles assembled with LFP (Sections 2 and 3). The lack of industrial recycling plants for reintroducing Li, C and PO_4^{3-} at the supply chain, concerns about the release of GHG and toxic gases and the high energy demand (usually from fossil fuels) at the pyrometallurgical processes draws attention to the need for technology development in the hydrometallurgical process of LFP batteries recycling. In the next sections, pre-treatments and pyrometallurgy for LIBs recycling will briefly be discussed. Then, literature studies on the hydrometallurgy recycling of $LiFePO_4$ batteries will be summarized and discussed in terms of environmental risks. The aqueous processing steps included were leaching and purification steps (precipitation, solvent extraction, ionic exchange, electrodialysis, ionic liquids and deep eutectic solvents).

6.2. Pre-Treatment

Batteries may follow the recycling route initially by pre-treatment stages, such as sorting, discharging, disassembling, dismantling and mechanical treatments [77]. A process designed to operate with LIBs may not support other battery types such as alkaline, NiMH, lead-acid and nickel-cadmium and may lead to effluent contamination and decreased efficiency. Sorting has two objectives: avoid contaminations by other types of batteries and separate LIBs by cathode chemistry [76].

The manual inspection has been used in LIBs recycling plants, and it is still the most common method in the EU [4]. The combination of automatic and mechanic sorting has been reported to separate LIBs, using techniques such as magnetic separation, X-ray fluorescence and electromagnetic and UV sorting [4,76,78].

After sorting, the spent LIBs must be completely discharged to avoid little residual power. If exposed to air when charged, short circuits may occur in the battery cells or packs, as well as liquid leakage, explosions or fires, leading to serious injuries for operators [78–80]. A method widely reported in the literature is submerging spent LIBs in saline solutions for a fast and low-cost discharge [10].

Discharged LIBs should be disassembled to isolate the cells and separate the main parts of the battery pack. This process efficiently recovers the aluminum household (or case),

copper electric wires, the printed circuit board, cooling systems and plastics from the battery pack. Dismantling separates the components of the cell: the aluminum shell, the cathode (aluminum foil and active material), the anode (copper foil and graphite) and the separator. For a large industrial scale, it should be necessary to automate processes or robots for the removal of internal cell components [78]. Releasing cells and separating inner components have challenges at a large scale: the automatic system should contemplate possible module and cell formats (cylindrical, prismatic and pouch) and cathode active materials.

For this reason, mechanical or comminution processes have been used in LIBs recycling to decrease the particles' size and change morphologies. There are several types of crushing equipment: shredders, hammer mills, balls mills and cutter mills. Beyond mechanical equipment, many techniques may be used: wet crushing, dry crushing, impact crushing and shear crushing [79]. Hammer mills break materials by fast-rotating hammers, shredding uses two rotating disks with a high torque and low speed and cutter mills use high-speed knives to cut materials [80].

Hammer mills are commonly used, and they were developed for the comminution of brittle materials (materials that fracture near to the elastic limit) [81]. Hammer mills shatter particles by impact crushing with the rotating hammers and striking them against the inner surface/breaker plate of the shell [82]. Waste materials are usually inhomogeneous; most of them show non-brittle behavior (metals, plastics, rubber, wood, paper and biomass) [83]. The comminution of non-brittle materials must contemplate mechanical processes: shearing, cutting, pulling, tearing and tensile stresses [84].

Shredders with horizontally mounted rotors have been used for the comminution of spent cars, and they are mainly employed to achieve material liberations of aluminum, lead-acid batteries and electronic scraps [85]. The shear shredder uses two opposing counter-rotating blades to cut or shear wastes, producing a higher uniformity in comparison with hammer mills [86].

Cutter mills are usually employed for fibrous materials, largely applied in the pulp and paper industry [87]. Based on cutting, shearing and impact grinding mechanisms, fine-grinding materials are achieved by material attrition with rotor blades [88]. The mechanical processing of LIBs using a knife mill has been reported to active material liberation, the separation of the less valuable fraction (plastics) and efficient metals leaching [89].

6.3. Pyrometallurgical Processing

Pyrometallurgy is well known as a process for recovering target metals at high temperatures (above 500 °C). The techniques widely applied for the treatment of batteries are smelting, roasting/calcination, incineration and pyrolysis. Microwave-assisted carbothermic reduction, smelting slag system design and salt-assisted roasting are under study [74,75].

In the smelting step, the batteries are heated above the metals and oxides melting point (up to 1400 °C), forming a liquid phase of molten alloys and another called a slag [75]. The degradation of organic compounds provides energy to raise the temperature and form the molten layers, while carbon and Al act as reducing agents. Valuable reduced metals are concentrated at the molten alloy phase. Pretreatment stages such as sorting and dismantling are negligible once the spent batteries are fed directly into a high-temperature furnace [74].

The roasting technique is a solid–gas reduction at temperatures above 600 °C. Unlike smelting, the reaction is conducted bellow the melting point temperature, and the objective is to reduce the metals to a lower valence stage for leaching efficiency improvement [74]. A roasting example is carbothermal reduction (CTR), which is used to repair the $LiFePO_4$ structure [75–79]. In carbothermic reduction, reductant carbonaceous materials are mixed with the cathode material and heated to 650–1000 °C. The main products of smelting and roasting techniques are metal alloys, slag, gases and precursors for the hydrometallurgical route [8].

Incineration consists in burn batteries cells or modules under oxygen atmosphere. Incineration has been applied as a pretreatment for battery modules releasing cells, reducing waste volume and removing plastics. Once applied in dismantled cells, it is capable of burning graphite, PE/PP polymers, PVDF and organic compounds at temperatures above 800 °C [90]. Pyrolysis burns material under inert atmosphere (N_2 or Ar) and seems to be an eco-friendlier process than incineration, considering the chemical compounds in LiBs [91]. For example, the pyrolysis of PE gives alkanes and alkenes, while PP gives a very small amount of its monomer during pyrolysis [92].

In the thermal treatment, the PDVF binder decomposes at 475 °C, releasing HF gases and short-chain hydrocarbons [93]. Furthermore, significant energy is demanded in order to maintain high temperatures, which release greenhouse gases. The Umicore pyrometallurgical process demands 5000 MJ per ton of processed batteries, mainly to maintain the temperature in ovens [94].

One of the main disadvantages of pyrometallurgy in LIBs recycling is the Li recovery, since it does not occur because the element goes through a slag phase which complicates its recovery, even by acid leaching. Above 1650 °C, Li forms volatile species, increasing its loss at the flue dust [94]. Moreover, the main products are metallic alloys, which are less profitable than the highly pure products obtained in hydrometallurgy processing [74].

6.4. Hydrometallurgical Processing of LFP Batteries

Hydrometallurgy routes involve processes for dissolving metals, mainly the cathode, by acid or alkali aqueous media, followed by separation and purification steps for obtaining the metallic compounds [95].

Compared with pyrometallurgy, aqueous processing demands lower energy and less GHG emissions (lower carbon footprint). In addition, organic compounds (PVDF and additives) are usually removed by solvents extraction or acid solution, preventing environmental contamination with toxic organic vapors and persistent organic pollutants from thermal degradation. On the other hand, final products are obtained as single-metal salts that are separated ($FePO_4$, $LiCO_3$, $Al(OH)_3$), which are more valuable than metallic alloys [8].

6.4.1. Leaching

Leaching depends on different parameters: stirring speed, solid/liquid ratio, acid concentration, temperature, time, reducing/oxidant agent and particle diameter. Several authors have studied the parameters for LFP cathode leaching, controlling the extraction percentage of metals. Two types of leaching for metal recovery are currently used: non-selective and selective recovery. The first technique recovers the whole cathode into the leach solution (such as Li, Fe and PO_4), while the selective recovery technique involves recovering Li from the leaching solution and $FePO_4$ as a leaching residue [96].

The literature supports the acid leaching with mineral (Table 3) and organic acids (Table 4). Among mineral acids, H_2SO_4 has the lowest price and high availability, and it has shown good results for industrial applications [97–100]. Table 3 depicts examples of acid leaching with H_2SO_4, where this mineral acid achieves up to 98% of LFP cathode leaching. Mineral acids have not shown selective properties in leaching, and the literature focuses on the recovery of all the metals. Despite that, the use of oxidizing agents (H_2O_2 and O_2) increases the selectivity towards Li leaching [101,102]. Equations (8) and (9) represent the non- and selective leaching of $LiFePO_4$ in H_2SO_4.

$$2LiFePO_{4(s)} + 3H_2SO_{4(aq)} \rightarrow FeSO_{4(aq)} + Li_2SO_{4(aq)} + 2H_3PO_{4(aq)} \quad (8)$$

$$2LiFePO_{4(s)} + H_2SO_{4(aq)} + H_2O_{2(aq)} \rightarrow FePO_{4(s)} \downarrow + Li_2SO_{4(aq)} + 2H_2O_{(aq)} \quad (9)$$

Table 3. Spent LFP cathode acid leaching treatment with the H_2SO_4 leaching agent, comparing the leaching efficiency among authors.

Pre-Treatment	Raw Material	Reagent	Conditions	Leaching Efficiency	Authors
Discharge	$LiFePO_4$ spent powder	2.5 mol/L H_2SO_4	Solid:liquid ratio 10 mL/g, 4 h, 60 °C and 500 rpm	Li = 97% Fe = 98%	[97]
Manual	$LiFePO_4$ spent powder	2 mol/L H_2SO_4	Solid:liquid ratio 20:1, 70 °C and 2 h	Li = 97.7% Fe = 93.3%	[99]
Separation	$LiFePO_4$ spent powder and Al foil	AMR (H_2SO_4 98%wt volume/mass spent LFP) = 0.35:1	20 °C, 90 min, Solid:liquid ratio 5:1 and 800 rpm	Li = 92.19% Fe = 91.53% P = 91.01% Al = 15.98%	[100]
Calcining (600 °C)	$LiFePO_4$ spent powder	10 g $LiFePO_4$ 0.32 mol/L H_2SO_4 H_2O_2	60 °C	Not mentioned	[103]
Discharge, Manual	$LiFePO_4$ spent powder	0.3 mol/L H_2SO_4, 2.07 H_2O_2/Li molar ratio	0.57 molar ratio H2SO4/Li, 200 rpm, 60 °C and 120 min	Li = 96.85% Fe = 0.03% P = 1.95%	[101]
Separation and Alkaline Leaching	$LiFePO_4$ spent powder	0.6 mol/L H_2SO_4 1.3 MPa O_2	Solid:liquid ratio 0.525:1, 120 °C and 90 min	Li = 97% Fe = 1%	[102]

Ref. [97] discharged and dismantled the LFP battery for the separation of electrodes sheets. Then, the authors crushed and heated the cathode sheet at 450–650 °C for the thermal degradation of the PVDF binder and the conductive carbon. The powder was separated from the Al metallic via an oscillating sieve and leached with H_2SO_4 in the absence of H_2O_2. The leaching efficiency was 97% Fe and 98% Li, using optimal leaching conditions: 2.5 mol/L H_2SO_4 concentration, solid-liquid ratio 10 mL/g, 60 °C and 4 h.

Ref. [99] evaluated the leaching performance of LFP spent powder in H_2SO_4 without H_2O_2. The H_2O_2 acts as an oxidizing agent, promoting the redox reaction Fe^{2+}/Fe^{3+} and $FePO_4$ precipitation. $LiFePO_4$ powder was obtained by the discharging, dismantling and alkaline leaching of the PVDF polymer (cathode immersed in 1 mol/L NaOH solution). The researchers reported a leaching efficiency of 96.67% Li and 93.25% Fe, under optimized conditions: 2 mol/L H_2SO_4, solid-liquid ratio 20:1, 70 °C and 2 h.

Ref. [100] leached a mixture of crushed LFP cathodes, without removing the Al sheet. The cells were dismantled to separate the cathode sheet and crushed. The optimal conditions that were selected were the higher leaching percentages of Li, Fe and P and the lower leaching efficiency for Al. The optimized leaching conditions were 20 °C, an AMR (analytical grade H_2SO_4 volume per mass of active material) of 0.35:1, a leaching time of 90 min, a liquid:solid ratio of 5:1 and a stirring speed of 800 rpm. The leaching efficiencies were 92.19% Li, 91.53% Fe, 91.01% P and 15.8% Al.

The aforementioned works focused on non-selective recovery, achieving leaching percentages above 90% for the target materials in LFP batteries (Li, Fe, PO_4 and Al foils). As presented in Table 3, a large quantity of the leaching agent (acid concentrations above 2 mol/L) is necessary to destroy the olivine structure [96]. A process designed to work with non-selective leaching may generate higher amounts of secondary waste, in terms of acid effluents. On the other hand, successive purification steps for separating metals from the solution enhance the reagents consumption for pH neutralization and result in a large amount of contaminated water.

Despite the poor selectivity, the addition of oxidizing agents to mineral acids may decrease Fe leaching. Ref. [101] demonstrated that the H_2SO_4 leaching controlled the stoichiometry ratio between the leaching agent and Li content and added an oxidizing

agent for Li selective extraction. The powder was obtained by discharging spent LFP batteries, dismantling to separate the cathode and immersing the cathode in a 0.4 mol/L NaOH solution for Al removal. Leaching experiments were carried out with 5 g of active material with different amounts of H_2SO_4 and H_2O_2, temperatures and leaching times. Under the optimized conditions (0.3 mol/L H_2SO_4, H_2O_2/Li molar ratio 2.07, H_2SO_4/Li molar ratio 0.57, 60 °C and 120 min), it extracted 96.85% of Li, 0.027% of Fe and 1.95% of P.

Ref. [102] reported an increase in the selectivity of H_2SO_4 by using O_2 as an oxidant agent. Spent $LiFePO_4$ batteries were pre-treated to remove Al and Cu and leached with H_2SO_4 and bubbling O_2. Leaching was carried out with the following conditions: 0.6 mol/L H_2SO_4, a 0.525:1 H_2SO_4/Li molar ratio, an O_2 partial pressure of 1.3 MPa, 120 °C and 90 min. At the best selectivity, 97% of the Li was leached, and more than 99% of the Fe was recovered at the residue as $FePO_4$ or $Fe_5(PO_4)_4(OH)_3.2H_2O$. Despite the increased selectivity with oxidizing agents, Fe and PO_4^{3-} impurities remain at the leaching solution, and the selective leaching has been better exploited with organic acids.

In addition to leaching studies using mineral acids, the literature has reported organic acids leaching because of availability and biocompatibility. Citric acid, oxalic acid and malic acid are commonly used because of their high and widespread content in the environment, produced by plant roots secretion, the metabolism of microorganisms and the decomposition of organic matter [104]. Organic acids have good selectivity and are usually employed to leach Li from $LiFePO_4$ spent cathodes.

Table 4 summarizes the leaching of the LFP cathode with organic acids. Some organic acids such as acetic acid (CH_3COOH), citric acid ($C_6H_8O_7$), maleic acid ($C_4H_4O_4$), formic acid (HCOOH) and oxalic acid ($C_2H_2O_4$) have been reported for the leaching of spent LFP cathodes. Studies report the use of organic acids for the selective leaching of Li, where $FePO_4$ remains at a solid state [98]. Equations (10) and (11) represent the Li leaching and $FePO_4$ solid formation, using citric and formic acid as leaching agents.

$$3H_3Cit_{(aq)} + 6LiFePO_{4(s)} + 3H_2O_{2(aq)} \rightarrow 6FePO_{4(s)} + 2Li_3Cit_{(aq)} + 6H_2O_{(aq)} \quad (10)$$

$$HCOOH_{(aq)} + LiFePO_{4(s)} + 1/2H_2O_2 \rightarrow HCOO^-{}_{(aq)} + Li^+{}_{(aq)} + 3FePO_{4(s)} \quad (11)$$

Table 4. Organic acids leaching of LFP batteries.

Pre-Treatment	Raw Material	Reagent	Conditions	Leaching Efficiency	Authors
Discharging, dismantling, manual cutting	Spent LFP cathode	2.5 mol/L H_2SO_4	120 g/L S/L ratio, 50 °C and 30 min	Li = 95.05% Selectivity = 94.8%	[95]
Discharging, dismantling, Alkaline leaching, crushing and sieving	$LiFePO_4$ spent powder	2 mol/L H_2SO_4	10% pulp density, 500 rpm, 30 °C and 30 min	Li = 90% Fe < 0.5%	[105]
Grinding	LFP battery	AMR (H_2SO_4 98%wt volume/mass spent LFP) = 0.35:1	300 rpm, 8 h grinding time and 25 BPR	Li = 97.82% Fe = 95.62%	[106]
Discharging, dismantling, cathode scrapped off, grounding and sieving	$LiFePO_4$ spent powder	10 g $LiFePO_4$ 0.32 mol/L H_2SO_4 H_2O_2	67 g/L S/L ratio and 90 min	Li = 94.8% Fe = 4.1% Al = 47.2% P = 0.8% Cu = 96.92%	[98]

Ref. [95] explored the use of CH_3COOH as a leaching agent for a selective Li extraction. Spent LFP batteries were discharged, immersing them in a 5%wt NaCl solution. The discharged batteries were dismantled in the cathode, anode, plastics and metal case. After 30 min, under conditions of 0.8 mol/L CH_3COOH, 6%vol. H_2O_2, 120 g/L S/L ratio and 50 °C,

the Li extraction was 95.05%. Comparing the Li extraction with the other metals leached, the ratio between the Li percentage and Fe percentage was 94.8% (selective leaching).

Ref. [105] explored the use of HCOOH for selective leaching. Spent LFP batteries were discharged in 1.0 mol/L NaCl solution and then dismantled. The cathode powder was separated from Al foils, immersing the cathode plates in 1.5%wt NaOH solution for 30 min under ultrasound with a 10% (*w*/*v*) pulp density. The cathode powder was washed with deionized water and dried at 60 °C for 48 h. The dried cathode material was crushed and sieved through a 74 µm sieve, and the fine cathode powder was leached. The optimized conditions were a 10% pulp density, HCOOH/Li molar ratio 3.23 with a 10% (*v*/*v*) solution of 50 wt% H_2O_2, 30 °C and 30 min. High-selectivity leaching has been achieved with 90% Li and 0.5% Fe.

Ref. [106] investigated the leaching with $C_6H_8O_7$ as a leaching agent. The leaching and grinding stages were carried out at the same time. The effects of the mass ratio of $C_6H_8O_7$ and LFP (10–80), the ball-to-powder ratio (BPR) (15–55 g/g), the volume of H_2O_2 (0–2 mL), the grinding time (0.5–4 h) and the rotation speed (100–500 rpm) were explored. The experimental results achieved optimal conditions of 25 BPR, 20 g/g $C_6H_8O_7$-to-LFP ratio, a BPR of 45, 8 h grinding time, 300 rpm rotation speed and 1 mL H_2O_2. The extraction efficiencies of Li and Fe were 97.82% and 3.86%, respectively.

Ref. [98] used natural sources of $C_6H_8O_7$ (apple, orange and lemon juices) as leaching agents. The spent LFP was pre-treated initially by discharging and dismantling. The cathode was separated manually, and the $LiFePO_4$ was separated from the Al foil. The black powder was ground and sieved. The lemon juice presented the best results, and the optimized conditions were 100% of lemon juice, 6 vol% of H_2O_2, S/L ratio of 67 g/L and 90 min. Selective leaching was achieved with 94.83% Li and 4.05% Fe.

Salt leaching was also reported in the literature [107], efficiently recovering Li without acid and avoiding secondary pollution. Ref. [108] applied salt leaching with a solution of $Fe_2(SO_4)_3$ in theoretical-molar dosage with the $LiFePO_4$ spent cathode. Spent batteries were first disassembled, removing the external plastic cases, and then dismantled and separated into cathode electrodes, anode electrodes, organic separators and plastic shells. The cathode scraps were mechanically separated from the Al foil by crushing, pulverizing and sieving. The spent LFP cathode leaching achieved an Li efficiency of 97.07%, even under a 500 g/L solid:liquid ratio (molar ratio $Fe_2(SO_4)_3$:$LiFePO_4$ = 1:2, at 28 °C for 30 min).

Ref. [107] demonstrated the leaching of a spent LFP cathode using an inexpensive salt $FeCl_3$ solution. Fe^{3+} substitutes Fe^{2+} at the $LiFePO_4$ structure, leaches Li^+ ions and forms $FePO_4$ precipitate. To simulate the $LiFePO_4$ spent cathode, the authors leached a commercial sample with a 97% mass of active material. It was necessary to use H_2O_2 in the proportion of 2:1 of LFP:H_2O_2 to attain Fe^{3+} oxidation. The best leaching conditions were a molar ratio of $FeCl_3$:$LiFePO_4$ 1:1, solid:liquid ratio of 300 g/L, 40 °C and 30 min of reaction time, whereas 99% Li leaching efficiency was obtained.

Beyond the environmental compatibility of organic acids, they have presented a higher performance for selective leaching than mineral acids. The environmentally friendly process is attained by three main characteristics: (1) selective recovery of Li promotes the one-step separation from $FePO_4$, (2) less secondary waste by the use of weak acid solutions and (3) less water contamination by purification steps.

6.4.2. Precipitation

Precipitation has been used for the purification and separation of metals, which consist of removing the metal ion from the solution using chemicals. The pH, redox potential, ionic activities and temperature influence the formation of insoluble species. Precipitation in aqueous media is controlled by standard Gibbs-Free Energy ($G_f°$). Based on $G_f°$, the Pourbaix Diagram may be plotted to indicate the predominant species formed and the possible solid products obtained. Figure 5 shows the Pourbaix Diagram of the Li–Fe–P–H_2O system at 25 °C. In redox potentials above 0 V, Fe is preferentially precipitated at pH 2 in the form of $FePO_4$ or in the hydroxide form of $Fe(OH)_3$ at pH 7. Insoluble Li species

such as Li_2CO_3 and Li_3PO_4 would precipitate by the addition of the reagents Na_2CO_3 or Na_3PO_4 [97,101,103].

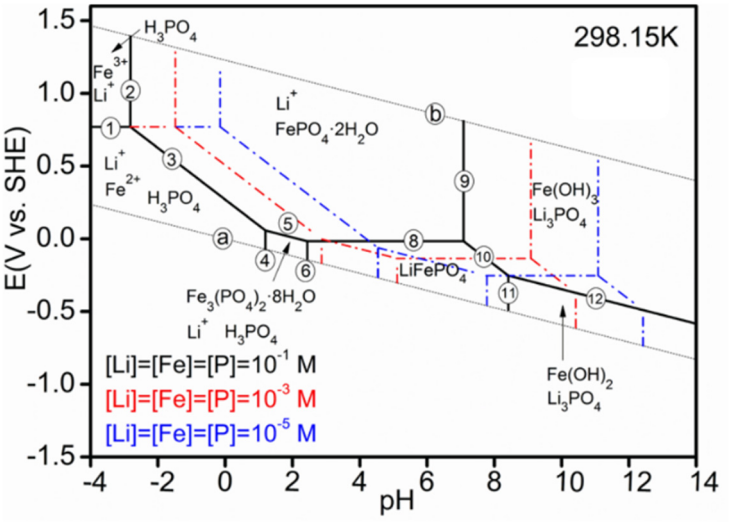

Figure 5. Pourbaix Diagram for the Li–Fe–P–H2O system at 25 °C [108].

Table 5 summarizes some precipitation processes applied to treat the leaching liquors of spent LFP batteries. Ref. [101] presented a purification process for the direct recovery of Li from H_2SO_4 leaching liquor. Li was selectively leached, and the concentration in the solution was 3.55 g/L Li, 1.72 mg/L Fe and 0.31 g/L P. Before leaching, the solution was heated to concentrate and achieved an Li concentration of 8.1 g/L. Stoichiometry $Na_3PO_4.12H_2O$ was introduced for Li_3PO_4 precipitation, following Equation (12), for 2 h at 250 rpm and 65 °C. The Li_3PO_4 precipitation efficiency was 95.6%.

$$3Li_2SO_4(aq) + 2Na_3PO_4(aq) \rightarrow 3Na_2SO_4(aq) + 2Li_3PO_4(s) \quad (12)$$

Table 5. Organic acids leaching of LFP batteries.

Purification Process	Reagent	Conditions	Purification Efficiency	Authors
Precipitation	NaOH Na_3PO_4	65 °C 2 h 250 rpm	Li_3PO_4 = 95.56%	[101]
Precipitation Regeneration	NH_3 Na_2CO_3 $LiCO_3$ $FePO_4$	Boil point Ball-milling, 7 h 300 °C, 4 h 700 °C, 10 h	Not mentioned	[97]
Resynthesis (Hydrothermal reaction)	Leachate liquor Li:Fe:P = 3:1:10 Glucose 8:100 weight ratio LFP cathode	200 °C, 6 h Filtration 50 °C, 8 h 200 °C, 6 h	Not mentioned	[99]
Precipitation	NaOH Na_3PO_4	Room temperature 240 min	Fe = 97.6% Li = 96.9%	[103]
Precipitation Regeneration	NaOH Na_2CO_3 $FePO_4$ $LiCO_3$ $C_6H_{12}O_6$	700 °C, 8 h Air and 700 °C, 3 h Air	Li = 84.8% Fe = 96.4%	[98]

Ref. [103] studied the precipitation process using, as precipitating agents, NaOH and Na_3PO_4. In the leaching liquor, 7.5 mL of 2.0 mol/L NaOH solution was added, and $FePO_4.H_2O$ precipitated. The remaining solution was evaporated, 1.0 mol/L Na_3PO_4 was added to the solution and Li_3PO_4 was recovered. The recovery rates of Fe and Li were 97.6% and 96.9%, respectively.

Figure 6 shows the Pourbaix Diagram for the Al–H_2O system at 25 °C. Up to pH 2, Al^{3+} is predominant, and it is commonly found in leach solutions from spent batteries treated with the Al foil [100]. After increasing the pH of the solution above 5, and in a wide range of Eh (−1.5 to 1.5 V), the predominant species is $Al(OH)_3$ (Figure 6). Ref. [109] precipitated insoluble $Al(OH)_3$ in a solution from acid mines drainage, using the precipitating agents NaOH, $Ca(OH)_2$ and Na_2CO_3, pH 5.5 and H_2O_2 addition, achieving Al precipitation percentages between 70.4 and 82.2%.

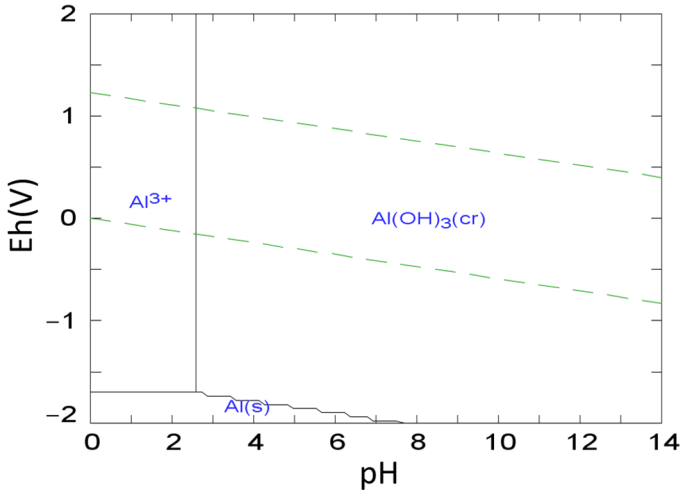

Figure 6. Pourbaix Diagram of the Al–H_2O system at 25 °C. Simulation in the software Hydra-medusa.

6.4.3. Solvent Extraction

Some solvents have been reported for the extraction of Li^+, Fe^{3+} and Al^{3+} from aqueous solutions such as di-(2-ethylhexyl)phosphoric acid (D2EHPA), tributyl phosphate (TBP) and malonamides [107,110–112].

Ref. [110] used four malonamides with phenyl and methyl groups as N,N′-substituents to extract Fe^{3+} from hydrochloric acid solutions. The removal of Fe(III) from the HCl solution may be used in leaching solutions of the spent LFP cathode in HCl. The extraction of Fe^{3+} from chloride solutions consists in the solvation of the $FeCl_3$ species by the solvent, and 90% Fe^{3+} extraction was obtained.

Ref. [111] studied the liquid–liquid extraction of lithium ions from aqueous solutions using the organic extractant di-(2-ethylhexyl)phosphoric acid (D_2EHPA), diluted into cyclohexane or TBP. Solvent extraction was carried out in batch and continuous experiments, and the results indicated an improved adsorption performance of microchannels when compared with conventional liquid–liquid extractors [111]. At the continuous process, the solvent and aqueous phases were mixed in a slug flow microreactor, composed of two syringe pumps connected to glass or a PTFE tube. By controlling the aqueous phase pH, the mixture achieves sludge flow at the tube and mass transfer coefficients of 1.62 to 2.48 1/s for Li^+ extraction. At the best condition, with an organic phase mixture of D2EHPA and TBP, flow through a PTFE tube, a pH of 11.9 and an extraction time of 10 s, more than 50% of the Li^+ was extracted to the organic phase.

Additionally, D2EHPA has been used to selectively remove Al^{3+} ions from spent Al-bearing $LiFePO_4$ cathodes leaching solution [113]. The organic phase was composed of D2EHPA and sulfonated kerosene, and the optimal conditions were a three-stage counter-current extraction experiment caried out at an aqueous-to-organic-phase ratio equal to 1

and 25 °C. The results showed that 96.4% of the aluminum was extracted, with only 1.1% Fe loss at the optimal conditions.

The organic extractant try-n-butyl phosphate (TBP), diluted in sulphonated kerosene, with a concentration of 3 mol/L of the extractant, has been used for Li and Fe separation from the aqueous phase [107]. Leach liquor from a selective salt leaching using $LiCl_3$ as the leaching agent was the aqueous phase, and it was mixed at the separator funnel and shaken mechanically for 10 min at 25 °C. The authors proposed a countercurrent solvent extraction in three stages, and after this process, 80% of the Li^+ and 80.34% of the Fe^{3+} were extracted as the [$LiFeCl_4$] complex to the organic phase. To provide an Li-rich solution, a one-stage stripping process with 6 mol/L HCl solution achieved a 60% Li stripping efficiency and less than 9 mg/L of Fe in the stripping solution, due to the $HFeCl_4$ complex at the organic phase. To increase the Li stripping to 90.23%, the aforementioned process has been carried out in five-stage countercurrent extraction, providing an Li-rich solution for precipitation as Li_2CO_3.

Confirming the outstanding capacity for selective Li extraction by the complex formation $FeCl_4^-$ on TBP, Ref. [114] studied extraction using TBP, with $FeCl_3$ as a co-extractant in kerosene. The aqueous phase was a synthetic solution simulating the LIBs waste leaching solution in HCl. Solvent extraction experiments were carried out in batch at the separation funnel, with an organic phase of 80% (v/v) TBP and 20% (v/v) kerosene and $FeCl_3$ at the aqueous phase, to promote the selective Li extraction. In single-stage extraction, with an O/A ratio = 1, and at 25 °C, the Li purity of the loaded organic phase was 65.6%. After organic phase washing and stripping with 6 mol/L HCl, the resulting Li solution contained 13.95 g/L and 99.1% purity.

The general downsides of solvent extraction are the concerns about environmental pollution (water, air and soil), the danger to the operator's health and the expensive purchase [115]. Common organic solvents are highly volatile, and during extraction, the extractant may depart the organic phase (extractant and diluent mixture) and enter the aqueous phase, called the "extractant dissolution" phenomenon [116].

The extractant dissolution increases the organic content of water, and in some cases, it can be toxic for human beings. The proposed mechanisms for extractant dissolution include the diffusion of the extractant into an aqueous phase, the formation of metal/extractant complexes and the return of complexes to an organic phase [117]. Further, other variables, such as the pH, type of metals, extractant/diluent weight ratio and solubility of the extractants, impact the extractant dissolution [116].

According to the New Jersey Department of Health, D2EHPA must be toxic by inhalation or absorption through the skin, it is a corrosive chemical and it causes breath diseases (NJDHSS, 2006). TBP can bioaccumulate and persists in environment as a pollutant. TBP is volatile and has become one of the most significant indoor air pollutants. In the aquatic environment, TBP bioaccumulates from water to fish and from fish to birds have been found in fish and bird muscle samples collected in Guangdong, China (Ma et al., 2013). Bioaccumulation increase concerns about toxicity in humans; epidemiologic studies have found that TBP is neurotoxic, and exposure is associated with DNA oxidative stress, reactive oxygen species (ROS) overproduction, the induction of DNA lesions and increased lactate dehydrogenase leakage [118].

6.4.4. Ionic Exchange Resins

Adsorption is a separation process by which one or more components in a fluid are transferred to the surface of a solid adsorbent [119]. The fluid is passed through a fixed bed of small solid particles, and the solid phase adsorbs the components until it is almost saturated, so the flow is stopped and the bed is regenerated by a desorption process. Ion exchange extracts metal ions from aqueous solutions and resembles techniques with adsorption processes [120]. In ion exchange, an insoluble solid phase previously bonded with cations or anions (adsorbent) is in contact with the ions of the solution (adsorbate), where ionic reactions replace ions between the solution and solid phase.

Ion-exchangers may be classified into four groups: (1) cationic resins with a strong acid exchange ability, (2) cationic resins with a weak acid exchange ability, (3) anionic resins with a strong base exchange ability and (4) anionic resins with a weak base exchange ability [121]. Common functional groups for the first category include the sulfonic acid group, and those for the second category include carboxylic acid groups. Regarding anionic resins, strong and weak base exchange properties are often due to quaternary ammonium groups and ammonium groups, respectively [121].

A variety of functional groups have been employed for water treatment, such as iminodiacetate, aminophosphonic, bispicolylamine, amidoxime, dithiocarbamate, 8-hydroxychinoline, diphosphonic, thiol and thiourea [122]. Ion exchange has a simple operation, low energy consumption and operation costs, a fast reaction, good cycling stability, simplicity in operation and easy post-treatment [123,124]. Additionally, it has resistance to temperature and physical degradation, along with reversible reactions, which allow for reuse many times [122].

Despite these advantages, only a few reports have described the application of the ion exchange method to the recycling of spent NCM-based cathodes or the purification of leaching solutions from mixed LIBs. Some ionic exchange techniques focus on removing transition metals such Ni, Co, Fe and Mn using chelating resins [125], and others focus on removing the Li by selective extraction [126,127].

Ref. [127] have shown ionic exchange with polycrystalline samples of $Cs_5K_4Fe_7(PO_4)_{10}$ for Li removal from an $LiNO_3$ solution and the production of the $Li_9Fe_7(PO_4)_{10}$ compound for electrode applications. The iron phosphate polycrystalline samples ($Cs_5K_4Fe_7(PO_4)_{10}$) were synthesized from the mixture of $(NH_4)H_2PO_4$, Fe_2O_3, Cs_2CO_3 and K_2CO_3, with a stoichiometric molar ratio of 10:3.5:2.5:2, at 750 °C for 2 days. Then, 100 mg of polycrystalline powders were immersed in 10 mL of the $LiNO_3$ solution at a 1 mol/L concentration for ionic exchange reaction. The reaction was carried out in hydrothermal conditions (200 °C), achieving 100% of Li^+ ion exchange and producing cathode material without pyrometallurgical regeneration methods, such as those discussed in previous sections.

As discussed previously, LFP cathode selective leaching is usually carried out to recover Li from scrapped cathode materials. Ref. [126] explored four kinds of H^+-form resins, among weak and strong acid cation exchange resins (with the functional groups carboxylic acid and sulfonic acid), to investigate Li-H ion exchange and its removal from oxalic acid, citric acid and H_2SO_4 leching solutions. Further, they explored ionic exchange in resins loaded with K ions (Li-K form) to recover Li and introduce K into a PO_4^{3-} stock solution. The studies indicated that resins with sulfonic acid functional groups are favorable for Li extraction, and the equilibrium capacity was calculated to be 14.5 and 6 mg of Li/g for the resin for the best condition and for the resin of the Li-H and Li-K ion exchange reaction.

Chelating resin with the aminomethylphosphonic functional group (Lewatit TP260) was capable of removing Fe, Al, Mn and Cu from the leach solution, while leaving valuable Co, Ni and Li [125]. A pure and high-value mixture in the raffinate with a battery grade was aimed for. The separation performance was higher at pH 3 and 60 °C, improving the purity and productivity. Despite the feasible and facile separation, the mineral acids did not efficiently elute the resin, and a two-step elution procedure was necessary. Cu and Mn are first removed with sulfuric acid, followed by Fe and Al removal with potassium oxalate. The suggested process produced pure Li-Co-Ni solution (battery grade—a > 99.6%), along with an Mn- and Cu-rich sulfuric acid solution and an oxalate solution of Fe–Al as by-products [125].

The commercial cationic chelating resin Purolite S950 (Purolite International Co., LTD) is composed of a polymer structure (styrene-divinylbenzene) with aminophosphonic functional groups. Phosphonic groups contain two types of active centers: phosphonic oxygen and hydroxyl acid groups (Equation (13)). The adsorption of transition elements ions proceeds via coordination bonds with phosphonic oxygen and ionic interaction with the hydroxyl groups [128]. Resin must require washing with acid solutions to convert the resin to the hydrogen form, using hydrochloric acid between 2 mol/L and 4 mol/L [129,130]. Aminophosphonic acid (AP) groups have presented good selectivity toward Fe^{3+}, achieving

loadings of 98% Fe^{3+} against 1% Ni^{2+} at 0.2 g resin/mL (Silva et al., 2019). Additionally, PuroliteS950 chelating resins have been used for Fe removal from phosphoric acid and nitric acid solutions with Al^{3+} ions, successfully removing 100% of Fe^{3+} [123].

$$HSO_4^- + R - NH - PO(OH)_{2,r} \rightleftarrows R - \left(NH_2^+ HSO_4^-\right) - PO(OH)_{2,r} \quad (13)$$

6.4.5. Electrodialysis

There are few reports about electrodialysis in LFP batteries recycling. Despite this, Li recovering using monovalent cation exchange membranes in electrodialysis has found application in recovering Li from Li_3PO_4 solutions and suspending $LiFePO_4$ in Li_2SO_4 solution.

Ref. [131] applied an electrodialysis system to separate Li from P in an Li_3PO_4 solution. Li3PO4 is the most insoluble Li specie, and to produce Li_2CO_3, it is necessary to separate Li from P. In this sense, it is possible to use, as the first purifying step in LFP, leaching solutions, separating Li from Fe and P. At 0.6 Ah and a current density of 184 A/m^2, throughout cation-exchange membranes (DuPont NAFION-117), authors have achieved a P interception rate of 95%.

Ref. [132] created a new process combining electrolysis and electrodialysis. The authors assembled a system with $LiFePO_4$ suspension in an Li_2SO_4 solution. The system has two electrodes in two chambers (the cathode and anode), where lithium ions could be released from spent LFP by a positive potential. The released lithium ion can migrate through a selective cation membrane to the cathode chamber, producing LiOH as a high-value product. Under the optimal conditions of a 60 mA/cm^2 current density, 50 g/L Li_2SO_4, 20 g/L LiOH and 100 g/L LFP, more than 96% of Li is leached without the addition of any chemical regents such as acid and oxidizing agents' consumptions, commonly used in hydrometallurgical processes.

6.4.6. Ionic Liquids

Ionic liquids (ILs) are composed of organic cations (C^+) and anions that can be organic or inorganic (A^-). The resulting salt (C^+A^-) has melting points below 100 °C [133]. Room temperature ionic liquids (RTILs) are an interesting class of solvents, basically by non-volatility and intrinsic ionic conductivity [134]. Ionic liquids should be used in four different manners: as the only extracting phase, as diluted in molecular solvents, as diluents for classical extractants and as an ionic exchange with ionic liquid cations (C^+) [112].

To the best of our knowledge, ionic liquids have not been used for the purification of leaching solutions of LFP batteries. Despite this, studies have used ionic liquids to extract lithium from aqueous solutions, resembling the techniques for the selective leaching of LFP cathode materials that produce lithium solution.

Ref. [112] showed the separation of lithium from LiCl solution using hydrophobic ionic liquid imidazolium. The classical extractant tri-n-butyl phosphate (TBP) was diluted in 1-ethyl-3-methylimidazolium *bis*(trifluoromethylsulfonyl)imide ([C_2mim] [Tf_2N])—imidazolium ionic liquid in different proportions to obtain an organic phase. The aqueous phase was obtained by dissolving lithium salts in HCl, HNO_3, DNO_3 and HTf_2N acid solutions. Solvent extraction was carried out at 25 °C, and the liquid–liquid mixture was shaken for 10 min at 1400 rpm in a thermo-shaker. The authors proved that by increasing the acidity of the aqueous solution, the Li extraction decreased, the IL cation C_2min^+ substituted Li^+ at the aqueous phase and the IL anion (Tf_2N) dissolved in the aqueous phase and was back-transferred to the organic phase with the TBP-Li^+ complex.

Ionic liquids have a usage cycle limit and subsequently become waste. Additionally, they have miscibility in water, presenting a threat to the aquatic environment and ecosystems [133].

6.4.7. Deep Eutectic Solvents

Deep eutectic solvents (DES) are considered cheap, wide sources, and they have biodegradability [135]. Further, the simple preparation of DES does not generate waste

and has no need for further purification steps [136]. DES stands out as an alternative for ionic liquids, which have a higher toxicity, challenging preparation and relatively higher cost [137].

DES is usually produced by mixing two components under heating, which produces a resulting mixture with a lower melting point than that of the pure substances. DES' raw materials may include metal chlorides such as $ZnCl_2$ and $FeCl_3$ (anidrous or hydrate), hydrogen bond acceptors (the most common being choline chloride) and hydrogen bond donors (glucose, urea, carboxylic acids and polyols) [135]. There are four types of DES: (1) metal chloride and quaternary ammonium salt, (2) metal chloride hydrate and quaternary ammonium salt, (3) hydrogen bond acceptors and hydrogen bond donors and (4) metal chloride and hydrogen bond donors [138].

The DES for LIBs recycling have been reported for the leaching of cathode materials as organic extractants and for PVDF binder removal. The application of DES specific to LFP batteries has not been carried out yet. Despite this, some works have used LCO and NMC batteries leaching [135] and separation to remove Fe(III) from mixed batteries leaching liquor [139]. In this sense, applications in Fe(III) solutions may be an analogous process to extraction from LFP leaching solutions.

Ref. [135] studied HDES for the extractive separation of Li(I), Co(II), Ni(II), Mn(II) and Fe(III) and subsequent recovery. Aliquat336 and L-menthol, the last environmentally friendly solvent, have been mixed, and the eutectic point was determined. The properties of the optimal proportion (3:7 Aliquat336/L-menthol molar ratio) and extraction profile for metals separation were determined. Extraction tests were carried out at 25 °C under atmospheric pressure and an O/A ratio of 1/5, and the phases were mixed at 35 rpm until the equilibrium. The aqueous phase was a leaching HCl solution of mixed metals. The results showed 99% recovery rates of Fe(III) for all the parameters studied, without Li coextraction. Thus, Aliquat 336/L-menthol-based HDES was used as the only extractant for efficient metal separation, without using volatile and toxic organic solvents.

Ref. [139] proposed a choline chloride–ethylene glycol deep eutectic solvent (ChCl:EG) for recovering cobalt from the electrode powder of end-of-life lithium-ion batteries (LIBs). The electrode powder included Fe impurities from physical treatments of LCO batteries, and the eutectic solvent was used to recover Co without Fe extraction. The aforementioned eutectic solvent was at 90 °C, and after 24 h of leaching, Cu was selective; additionally, a second leaching with the same mixture at 180 °C and 20 h leached Co and Mn, and in both processes, Fe impurities remained at the solid state. As Fe(III) is a commonly known impurity in LIBs hydrometallurgical processing, this process may separate Fe and increase the purity of other batteries.

7. Conclusions

LIBs stand out in applications such as portable electronic devices and electric vehicles, as they are the main technology in electric storage. Advances in $LiFePO_4$ batteries have gained priority in recent years. China, as the largest electric vehicles market in 2022, forecasts a high waste production only from LFP spent batteries. Secondary production by recycling end-of-life LFP batteries must recover critical materials such as Li, C(graphite) and PO_4^{3-}, reduce the incorrect disposal and release toxic chemicals to the environment [140]. The intrinsic downsides of the pyrometallurgical processes, combined with the scarcity of hydrometallurgical industrial processes around the world, increase the demand for new recycling processes based on aqueous processing for a lower carbon footprint and environmental protection.

In hydrometallurgical processing, the choice of organic acids with a higher environmental compatibility for selective Li leaching has shown the reduced consumption of chemical reactants and fewer purification steps, which reduces the effluent pollution. Classical purification steps such as precipitation and solvent extraction increase the chemical consumption and aqueous pollution. Organic extractants (D_2EHPA and TBP) have a high toxicity and must persist in the environment. For these reasons, alternative ionic

exchange, electrodialysis, ionic liquids and deep eutectic solvents steps have been proposed to make recycling environmentally friendly, with a decreased energy demand and decreased secondary pollution.

Author Contributions: Conceptualization, methodology, formal analysis, investigation, data curation, writing—original draft preparation, D.d.S.V., A.B.B.J., D.C.R.E. and J.A.S.T.; writing—review and editing, D.d.S.V. and A.B.B.J. All authors have read and agreed to the published version of the manuscript.

Funding: The authors would like to acknowledge the Fundação de Amparo à Pesquisa do Estado de São Paulo and Capes (grants: 2012/51871/9, 2019/11866-5, 2020/00493-0 and 2021/14842-0 São Paulo Research Foundation) for the financial support. This project was developed with the support of SemeAd (FEAUSP), FIA Fundação Instituto de Administração and Cactvs Instituto de Pagamento S.A. through the granting of assistance to the research project Bolsa SemeAd PQ Jr (Public Notice 2021.01).

Institutional Review Board Statement: Not applicable.

Informed Consent Statement: Not applicable.

Data Availability Statement: Not applicable.

Conflicts of Interest: The authors declare no conflict of interest.

References

1. Ali, H.; Khan, H.; Pecht, M. Circular economy of Li Batteries: Technologies and trends. *J. Energy Storage* **2022**, *40*, 102690. [CrossRef]
2. Zhao, Y.; Pohl, O.; Bhatt, A.; Collis, G.; Mahon, P.; Ruther, T.; Hollenkamp, A. A Review on Battery Market Trends, Second-Life Reuse, and Recycling. *Sustain. Chem.* **2021**, *2*, 167–205. [CrossRef]
3. Pandey, A.; Patnaik, S.; Pati, S. Available technologies for remanufacturing, repurposing, and recycling lithium-ion batteries: An introduction. In *Nano Technology for Battery Recycling, Remanufacturing, and Reusing*; Elsevier: New Delhi, India, 2022; Volume 1, p. 33.
4. Windisch-Kern, S.; Gerold, E.; Nigl, T.; Jandric, A.; Altendorfer, M.; Rutrecht, B.; Scherhaufer, S.; Raupenstrauch, H.; Pomberger, R.; Antrekowitsch, H.; et al. Recycling chains for lithium-ion batteries: A critical examination of current challenges, opportunities and process dependencies. *Waste Manag.* **2022**, *138*, 125–139. [CrossRef]
5. Sharma, I.; Chandel, M. Will electric vehicles (EVs) be less polluting than conventional automobiles under Indian city conditions? *Case Stud. Transp. Policy* **2020**, *8*, 1489–1503. [CrossRef]
6. Yuan, H.; Wang, X.; Wu, Q.; Shu, H.; Yang, X. Effects of Ni and Mn doping on physicochemical and electrochemical performances of $LiFePO_4$/C. *J. Alloys Compd.* **2017**, *675*, 187–194. [CrossRef]
7. Miao, Y.; Hynan, P.; Jouanne, A.; Yokochi, A. Current Li-Ion Battery Technologies in Electric Vehicles and Opportunities for Advancements. *Energies* **2019**, *12*, 1074. [CrossRef]
8. Harper, G.; Sommerville, R.; Kendrick, E.; Driscoll, L.; Slater, P.; Stolkin, R.; Walton, A.; Christensen, P.; Heidrich, O.; Lambert, S.; et al. Recycling lithium-ion batteries from electric vehicles. *Nature* **2019**, *575*, 75. [CrossRef] [PubMed]
9. Mohanty, A.; Sahu, S.; Sukla, L.; Devi, N. Application of various processes to recycle lithium-ion batteries (LIBs): A brief review. *Mater. Today Proc.* **2021**, *47*, 1203–1212. [CrossRef]
10. Martins, L.S.; Guimarães, L.F.; Botelho Junior, A.B.; Tenório, J.A.S.; Espinosa, D.C.R. Electric car battery: An overview on global demand, recycling and future approaches towards sustainability. *J. Environ. Manag.* **2021**, *295*, 113091. [CrossRef]
11. Jung, J.; Sui, P.; Zhang, J. A review of recycling spent lithium-ion battery cathode materials using hydrometallurgical treatments. *J. Energy Storage* **2021**, *35*, 102217. [CrossRef]
12. Ma, Z.; Shao, G.; Fan, Y.; Wang, G.; Song, J.; Liu, T. Tunable Morphology Synthesis of $LiFePO_4$ Nanoparticles as Cathode Materials for Lithium Ion Batteries. *Appl. Mater. Interfaces* **2014**, *6*, 9236–9244. [CrossRef]
13. Xu, G.; Li, F.; Tao, Z.; Wei, X.; Liu, Y.; Li, X.; Ren, Z.; Shen, G.; Han, G. Monodispersed $LiFePO_4$@C core–shell nanostructures for a high power Li-ion battery cathode. *J. Power Sources* **2014**, *246*, 696–702. [CrossRef]
14. Pender, J.P.; Jha, G.; Youn, D.H.; Ziegler, J.M.; Andoni, I.; Choi, E.J.; Heller, A.; Dunn, B.S.; Weiss, P.S.; Penner, R.M.; et al. Electrode Degradation in Lithium-Ion Batteries. *ACS Nano* **2020**, *14*, 1243–1295. [CrossRef]
15. Zheng, J.; Ye, Y.; Pan, F. 'Structure units' as material genes in cathode materials for lithium-ion batteries. *Natl. Sci. Rev.* **2020**, *17*, 242. [CrossRef]
16. Zhang, B.; Wang, S.; Li, Y.; Sun, P.; Yang, C.; Wang, D.; Liu, L. Review: Phase transition mechanism and supercritical hydrothermal synthesis of nano lithium iron phosphate. *Ceram. Int.* **2020**, *46*, 27922–27939. [CrossRef]
17. Tolganbek, N.; Yerkinbekova, Y.; Kalybekkyzy, S.; Bakenov, Z.; Mentbayeva, A. Current state of high voltage olivine structured $LiMPO_4$ cathode materials for energy storage applications: A review. *J. Alloys Compd.* **2021**, *882*, 160774. [CrossRef]
18. Bhuvaneswari, D.; Kalaiselvi, N. In situ carbon coated $LiFePO_4$/C microrods with improved lithium intercalation behavior. *Phys. Chem. Chem. Phys.* **2014**, *16*, 1469–1478. [CrossRef] [PubMed]

19. Zhao, N.; Li, Y.; Zhao, X.; Zhi, X.; Liang, G. Effect of particle size and purity on the low temperature electrochemical performance of $LiFePO_4$/C cathode material. *J. Alloys Compd.* **2016**, *683*, 123–132. [CrossRef]
20. Statista, Different Types of EV Batteries' Market Share Worldwide 2020–2050. 2020. Available online: https://www.statista.com/studies-and-reports/industries-and-markets (accessed on 10 January 2023).
21. Forte, F.; Pietrantonio, M.; Pucciarmati, S.; Puzone, M.; Fontana, D. Lithium iron phosphate batteries recycling: An assessment of current status. *Crit. Rev. Environ. Sci. Technol.* **2020**, *51*, 2232–2259. [CrossRef]
22. Oh, S.; Huang, Z.; Zhang, B.; Yu, Y.; He, Y.; Kim, J. Low temperature synthesis of graphene-wrapped $LiFePO_4$ nanorod cathodes by the polyol method. *J. Mater. Chem.* **2012**, *22*, 17215. [CrossRef]
23. Yuan, C.; Deng, Y.; Li, T.; Yang, F. Manufacturing energy analysis of lithium ion battery pack for electric vehicles. *CIRP Ann.* **2017**, *66*, 53–56. [CrossRef]
24. Sui, D.; Si, L.; Li, G.; Yang, Y.; Zhang, Y.; Yan, W. A Comprehensive Review of Graphene-Based Anode Materials for Lithium-ion Capacitors. *Chemistry* **2021**, *3*, 1215–1246. [CrossRef]
25. Sandhya, C.; John, B.; Gouri, C. Lithium titanate as anode material for lithium-ion cells: A review. *Ionics* **2014**, *20*, 601–620. [CrossRef]
26. Costa, C.; Lanceros-Mendez, S. Recent advances on battery separators based on poly(vinylidene fluoride) and its copolymers for lithium-ion battery applications. *Curr. Opin. Electrochem.* **2021**, *29*, 100752. [CrossRef]
27. Li, X.; Tao, J.; Hu, D.; Engelhard, M.; Zhao, W.; Zhang, J.; Xu, W. Stability of polymeric separators in lithium metal batteries in a low voltage environment. *J. Mater. Chem. A* **2018**, *6*, 5006. [CrossRef]
28. Jang, J.; Oh, J.; Jeong, H.; Kang, W.; Jo, C. A Review of Functional Separators for Lithium Metal Battery Applications. *Materials* **2020**, *13*, 4625. [CrossRef]
29. Costa, C.; Lizundia, E.; Lanceros-Mendez, S. Polymers for advanced lithium-ion batteries: State of the art and future needs on polymers for the different battery components. *Prog. Energy Combust. Sci.* **2020**, *79*, 100846. [CrossRef]
30. Li, Y.; Pu, H.; Wei, Y. Polypropylene/polyethylene multilayer separators with enhanced thermal stability for lithium-ion battery via multilayer coextrusion. *Electrochim. Acta* **2018**, *264*, 140–149. [CrossRef]
31. Aumnate, C.; Rudolph, N.; Samadi, M. Recycling of Polypropylene/Polyethylene Blends: Effect of Chain Structure on the Crystallization Behaviors. *Polymers* **2019**, *11*, 1456. [CrossRef]
32. Demeuse, M.T. Ceramic-coated separators. In *Polymer-Based Separators for Lithium-Ion Batteries*, 1st ed.; Elsevier: Ghangzhou, China, 2021; pp. 115–138.
33. Shi, C.; Dai, J.; Xiu, S.; Peng, L.; Li, C.; Wang, X.; Zhang, P.; Zhao, J. A high-temperature stable ceramic-coated separator prepared with polyimide binder/Al2O3 particles for lithium-ion batteries. *J. Membr. Sci.* **2016**, *517*, 91–99. [CrossRef]
34. Miranda-Quintana, R.; Smiatek, J. Beneficial properties of solvents and ions for lithium ion and post-lithium ion batteries: Implications from charge transfer models. *Electrochim. Acta* **2021**, *384*, 138418. [CrossRef]
35. Diederichsen, K.; Mcshane, E.; Mccleskey, B. Promising Routes to a High Li^+ Transference Number Electrolyte for Lithium Ion Batteries. *ACS Energy Lett.* **2017**, *2*, 2563–2575. [CrossRef]
36. Qiao, S.; Meng, X.; Cao, W.; Yu, S.; Liu, C.; Huang, Q. Effect of lithium salts LiPF6 and LiBF4 on combustion properties of electrolyte with EC/PC/EMC under different pressures. *Case Stud. Therm. Eng.* **2022**, *30*, 101741. [CrossRef]
37. Xu, K. Nonaqueous Liquid Electrolytes for Lithium-Based Rechargeable Batteries. *Chem. Rev.* **2004**, *104*, 4303–4411. [CrossRef]
38. Schaffner, B.; Schaffner, F.; Verevkin, S.P.; Borner, A. Organic Carbonates as Solvents in Synthesis and Catalysis. *Chem. Rev.* **2010**, *110*, 4554–4581. [CrossRef] [PubMed]
39. Nomanbhay, S.; Ong, M.; Chew, K.; Show, P.; Lam, M.; Chen, W. Organic Carbonate Production Utilizing Crude Glycerol Derived as By-Product of Biodiesel Production: A Review. *Energies* **2020**, *13*, 1483. [CrossRef]
40. Zhang, S.; Jow, T.; Amine, K.; Henriksen, G. $LiPF_6$-EC-EMC electrolyte for Li-ion battery. *J. Power Sources* **2002**, *107*, 18–23. [CrossRef]
41. Kim, K.; Cho, J.; Hwang, J.; Im, J.; Lee, Y. A key strategy to form a LiF-based SEI layer for a lithium-ion battery anode with enhanced cycling stability by introducing a semi-ionic C-F bond. *J. Ind. Eng. Chem.* **2021**, *99*, 48–54. [CrossRef]
42. Heng, S.; Lv, L.; Zhiu, Y.; Shao, J.; Huang, W.; Long, F.; Qu, Q.; Zheng, H. Organic salts with unsaturated bond and diverse anions as substrates for solid electrolyte interphase on graphite anodes. *Carbon* **2021**, *183*, 108–118. [CrossRef]
43. Delaporte, N.; Perea, A.; Paolella, A.; Dubé, J.; Vigeant, M.; Demers, H.; Clément, D.; Zhu, W.; Gariépy, V.; Zaghib, K. Alumina-flame retardant separators toward safe high voltage Li-Ion batteries. *J. Power Sources* **2021**, *506*, 230189. [CrossRef]
44. Zhang, F.; Hu, X.; Langari, R.; Cao, D. Energy management strategies of connected HEVs and PHEVs: Recent progress and outlook. *Prog. Energy Combust. Sci.* **2019**, *73*, 235–256. [CrossRef]
45. Global EV Outlook 2022. International Energy Agency. 2022. Available online: www.iea.org (accessed on 20 January 2023).
46. Global EV Outlook 2021. International Energy Agency. 2021. Available online: www.iea.org (accessed on 20 January 2023).
47. Li, J.; Yang, B. Analysis of greenhouse gas emissions from electric vehicle considering electric energy structure, climate and power economy of ev: A China case. *Atmos. Pollut. Res.* **2020**, *11*, 1–11. [CrossRef]
48. Norwegian Ministry of Climate and Environment, Norway's National Plan. 2019. Available online: https://www.regjeringen.no/contentassets/4e0b25a4c30140cfb14a40f54e7622c8/national-plan-2030_version19_desember.pdf (accessed on 20 January 2023).
49. Quan, J.; Zhao, S.; Song, D.; Wang, T.; He, W.; Li, G. Comparative life cycle assessment of LFP and NCM batteries including the secondary use and different recycling technologies. *Sci. Total Environ.* **2022**, *819*, 153105. [CrossRef]

50. Mossali, E.; Picone, N.; Gentilini, L.; Rodriguez, O.; Pérez, J.; Colledani, M. Lithium-ion batteries towards circular economy: A literature review of opportunities and issues of recycling treatments. *J. Environ. Manag.* **2020**, *264*, 110500. [CrossRef]
51. Miao, Y.; Liu, L.; Zhang, Y.; Tan, Q.; Li, J. An overview of global power lithium-ion batteries and associated critical metal recycling. *J. Hazard. Mater.* **2022**, *425*, 127900. [CrossRef] [PubMed]
52. Chen, B.; Liu, M.; Cao, S.; Hu, H.; Chen, G.; Guo, X.; Wang, X. Direct regeneration and performance of spent LiFePO4 via a green efficient hydrothermal technique. *J. Alloys Compd.* **2022**, *924*, 166487. [CrossRef]
53. United States Geological Survey, Mineral Commodity Summary. 2019. Available online: https://www.usgs.gov/ (accessed on 20 January 2023).
54. Olivetti, E.; Ceder, G.; Gaustad, G.; Fu, X. Lithium-Ion Battery Supply Chain Considerations: Analysis of Potential Bottlenecks in Critical Metals. *Joule* **2017**, *1*, 229–243. [CrossRef]
55. Rui, X.; Geng, Y.; Sun, X.; Hao, H.; Xiao, S. Dynamic material flow analysis of natural graphite in China for 2001–2018. *Resour. Conserv. Recycl.* **2021**, *173*, 105732. [CrossRef]
56. Spears, B.; Brownlie, W.; Cordell, D.; Hermann, L.; Mogollón, J. Concerns about global phosphorus demand for lithium-iron-phosphate batteries in the light electric vehicle sector. *Commun. Mater.* **2020**, *14*, 3. [CrossRef]
57. Ministry of Natural Resources, China Mineral Resources. 2022. Available online: https://www.mnr.gov.cn/sj/sjfw/kc_19263/zgkczybg/202209/P020220921322252399161.pdf (accessed on 20 January 2023).
58. Cabello, J. Lithium brine production, reserves, resources and exploration in Chile: An updated review. *Ore Geol. Rev.* **2021**, *128*, 103883. [CrossRef]
59. United States Geological Survey, Mineral Commodity Summary. 2022. Available online: https://www.usgs.gov/ (accessed on 20 January 2023).
60. Martim, G.; Rentsch, L.; Hock, M.; Bertau, M. Lithium market research—*Global* supply, future demand and price development. *Energy Storage Mater.* **2017**, *6*, 171–179. [CrossRef]
61. Zeng, X.; Li, J. Spent rechargeable lithium batteries in e-waste: Composition and its implications. *Front. Environ. Sci. Eng.* **2014**, *8*, 792–796. [CrossRef]
62. European Comission, Critical Raw Materials Resilience: Charting a Path towards Greater Security and Sustainability. 2019. Available online: https://commission.europa.eu/index_en/ (accessed on 21 January 2023).
63. Government of Canada, Natural Resources Canada. 2022. Available online: https://nrcan.gc.ca/ (accessed on 21 January 2023).
64. Sridhar, S.; Salkuti, R. Development and future scope of renewable energy and energy storage systems. *Smart Cities* **2022**, *5*, 668–699. [CrossRef]
65. Ministério da Ciência, Tecnologia, Inovações e Comunicações (MCTIC), Estratégia Nacional de Ciência, Tecnologia e Inovação. 2016. Available online: http://www.mcti.gov.br/ (accessed on 21 January 2023).
66. Castro, F.; Peiter, C.; Góes, G. Minerais estratégicos e as relações entre brasil e china: Oportunidades de cooperação para o desenvolvimento da indústria mineral brasileira. *RTM* **2020**, *24*, 349–378.
67. Kang, D.; Chen, M.; Ogunseitan, O.A. Potential Environmental and Human Health Impacts of Rechargeable Lithium Batteries in Electronic Waste. *Environ. Sci. Technol.* **2013**, *47*, 5495–5503. [CrossRef]
68. Nie, H.; Xu, L.; Song, D.; Song, J.; Shi, X.; Wang, X.; Zhang, L.; Yuan, Z. $LiCoO_2$: Recycling from spent batteries and regeneration with solid state synthesis. *Green Chem.* **2015**, *17*, 1276–1280. [CrossRef]
69. Lai, X.; Huang, Y.; Deng, C.; Gu, H.; Han, X.; Zheng, Y.; Ouyang, M. Sorting, regrouping, and echelon utilization of the large-scale retired lithium batteries: A critical review. *Renew. Sustain. Energy Rev.* **2021**, *146*, 111162. [CrossRef]
70. Velázquez-Martínez, O.; Valio, J.; Santasalo-Aarnio, A.; Reuter, M.; Serna-Guerrero, R. A Critical Review of Lithium-Ion Battery Recycling Processes from a Circular Economy Perspective. *Batteries* **2019**, *5*, 68. [CrossRef]
71. Pagliaro, M.; Meneguzzo, F. Lithium battery reusing and recycling: A circular economy insight. *Heliyon* **2019**, *5*, 1866. [CrossRef]
72. Lima, M.; Pontes, L.; Vasconcelos, A.; Junior, W.; Wu, K. Economic Aspects for Recycling of Used Lithium-Ion Batteries from Electric Vehicles. *Energies* **2022**, *15*, 2203. [CrossRef]
73. Fan, E.; Li, L.; Wang, Z.; Lin, J.; Huang, Y.; Yao, Y.; Chen, R.; Wu, F. Sustainable Recycling Technology for Li-Ion Batteries and Beyond: Challenges and Future Prospects. *Chem. Rev.* **2020**, *120*, 7020–7063. [CrossRef] [PubMed]
74. Makuza, B.; Tian, Q.; Guo, X.; Chattopadhyay, K.; Yu, D. Pyrometallurgical options for recycling spent lithium-ion batteries: A comprehensive review. *J. Power Sources* **2021**, *491*, 229622. [CrossRef]
75. Liu, C.; Lin, J.; Cao, H.; Zhang, Y.; Sun, Z. Recycling of spent lithium-ion batteries in view of lithium recovery: A critical review. *J. Clean. Prod.* **2019**, *228*, 801–813. [CrossRef]
76. Larouche, F.; Tedjar, F.; Amouzegar, K.; Houlachi, G.; Bouchard, P.; Demopoulos, G.; Zaghib, K. Progress and Status of Hydrometallurgical and Direct Recycling of Li-Ion Batteries and Beyond. *Materials* **2020**, *13*, 801. [CrossRef] [PubMed]
77. Tian, G.; Yuan, G.; Aleksandrov, A.; Zhang, T.; Li, Z.; Fathollahi-Fard, A.; Ivanov, M. Recycling of spent Lithium-ion Batteries: A comprehensive review for identification of main challenges and future research trends. *Sustain. Energy Technol. Assess.* **2022**, *53*, 102447. [CrossRef]
78. Roy, J.; Cao, B.; Madhavi, S. A review on the recycling of spent lithium-ion batteries (LIBs) by the bioleaching approach. *Chemosphere* **2021**, *282*, 130944. [CrossRef]
79. Sommerville, R.; Shaw-Stewart, J.; Goodship, V.; Rowson, N.; Kendrick, E. A review of physical processes used in the safe recycling of lithium ion batteries. *Sustain. Mater. Technol.* **2020**, *25*, 197. [CrossRef]

80. Lai, X.; Huang, Y.; Gu, H.; Deng, C.; Han, X.; Feng, X.; Zheng, Y. Turning waste into wealth: A systematic review on echelon utilization and material recycling of retired lithium-ion batteries. *Energy Storage Mater.* **2021**, *40*, 96–123. [CrossRef]
81. Eisenlauer, M.; Teipel, U. Comminution energy and particulate properties of cutting and hammer-milled beech, oak, and spruce wood. *Powder Technol.* **2021**, *394*, 685–704. [CrossRef]
82. Dey, S.K.; Dey, S.; Das, A. Comminution features in an impact hammer mill. *Powder Technol.* **2013**, *235*, 914–920. [CrossRef]
83. Schubert, G.; Bernotat, S. Comminution of non-brittle materials. *Int. J. Miner. Process.* **2004**, *74*, 19–30. [CrossRef]
84. Rácz, A.; Csoke, B. Comminution of single real waste particles in a swing-hammer shredder and axial gap rotary shear. *Powder Technol.* **2021**, *390*, 182–189. [CrossRef]
85. Kichner, J.; Timmel, G.; Schubert, G. Comminution of metals in shredders with horizontally and vertically mounted rotors—microprocesses and parameters. *Powder Technol.* **1999**, *105*, 274–281. [CrossRef]
86. Luo, S.; Xiao, B.; Hu, Z.; Liu, S.; Guo, X. An experimental study on a novel shredder for municipal solid waste (MSW). *Int. J. Hydrog. Energy* **2009**, *34*, 1270–1274. [CrossRef]
87. Vikharev, S. Engineering of the knife grinding machine milling process. In *IOP Conference Series: Materials Science and Engineering*; IOP Publishing: Bristol, UK, 2018; Volume 450.
88. Yokoyama, T.; Inoue, Y. Selection of Fine Grinding Mills. *Handb. Powder Technol.* **2007**, *12*, 487–508.
89. Guimarães, L.; Botelho Junior, A.; Espinosa, D.C.R. Sulfuric acid leaching of metals from waste Li-ion batteries without using reducing agent. *Miner. Eng.* **2022**, *183*, 107597. [CrossRef]
90. Lee, C.; Rhee, K. Preparation of $LiCoO_2$ from spent lithium-ion batteries. *J. Power Sources* **2002**, *109*, 17–21. [CrossRef]
91. Ekberg, C.; Petranikova, M. Lithium Batteries Recycling. In *Lithium Process Chemistry*, 1st ed.; Elsevier: Amsterdam, The Netherlands, 2015; pp. 233–267.
92. Zevenhoven, R.; Karlsson, M.; Hupa, M.; Frankenhaeuser, M. Combustion and Gasification Properties of Plastics Particles. *J. Air Waste Manag. Assoc.* **1997**, *47*, 861–870. [CrossRef]
93. Wang, M.; Liu, K.; Dutta, S.; Alessi, D.; Rinklebe, J.; Ok, Y.; Tsang, D. Recycling of lithium iron phosphate batteries: Status, technologies, challenges, and prospects. *Renew. Sustain. Energy Rev.* **2022**, *163*, 112215. [CrossRef]
94. Hu, X.; Mousa, E.; Tian, Y.; Ye, G. Recovery of Co, Ni, Mn, and Li from Li-ion batteries by smelting reduction—Part I: A laboratory-scale study. *J. Power Sources* **2021**, *483*, 228936. [CrossRef]
95. Yang, Y.; Meng, X.; Cao, H.; Lin, X.; Liu, C.; Sun, Y.; Zhang, Y.; Sun, Z. Selective recovery of lithium iron phosphate batteries: A sustainable process. *Green Chem.* **2018**, *20*, 3121–3133. [CrossRef]
96. Kumar, J.; Neiber, R.; Park, J.; Soomro, R.; Greene, G.; Mazari, S.; Seo, H.; Lee, J.; Shon, M.; Chang, D.; et al. Recent progress in sustainable recycling of $LiFePO_4$-type lithium-ion batteries: Strategies for highly selective lithium recovery. *Chem. Eng. J.* **2022**, *431*, 133993. [CrossRef]
97. Zheng, R.; Zhao, L.; Wang, W.; Liu, Y.; Ma, Q.; Mu, D.; Li, R.; Dai, C. Optimized Li and Fe recovery from spent lithium-ion batteries via a solution-precipitation method. *R. Soc. Chem. Adv.* **2016**, *6*, 43613. [CrossRef]
98. Kumar, J.; Shen, X.; Li, B.; Liu, H.; Zhao, J. Selective recovery of Li and $FePO_4$ from spent $LiFePO_4$ cathode scraps by organic acids and the properties of the regenerated $LiFePO_4$. *Waste Manag.* **2020**, *113*, 32–40. [CrossRef]
99. Song, Y.; Xie, B.; Song, S.; Lei, S.; Sun, W.; Xu, R.; Yang, Y. Regeneration of $LiFePO_4$ from spent lithium-ion batteries via a facile process featuring acid leaching and hydrothermal synthesis. *Green Chem.* **2021**, *23*, 3963. [CrossRef]
100. Lou, W.; Zhang, Y.; Zhang, Y.; Zheng, S.; Sun, P.; Wang, X.; Li, J.; Qiao, S.; Zhang, Y.; Wenzel, M.; et al. Leaching performance of Al-bearing spent $LiFePO_4$ cathode powder in H_2SO_4 aqueous solution. *Trans. Nonferrous Met. Soc. China* **2021**, *31*, 817–831. [CrossRef]
101. Li, H.; Xing, S.; Liu, Y.; Li, F.; Guo, H.; Kuang, G. Recovery of Lithium, Iron, and Phosphorus from Spent $LiFePO_4$ Batteries Using Stoichiometric Sulfuric Acid Leaching System. *ACS Sustain. Chem. Eng.* **2017**, *5*, 8017–8024. [CrossRef]
102. Wu, D.; Wang, D.; Liu, Z.; Rao, S.; Zhang, K. Selective recovery of lithium from spent lithium iron phosphate batteries using oxidation pressure sulfuric acid leaching system. *Trans. Nonferrous Met. Soc. China* **2022**, *32*, 2071–2079. [CrossRef]
103. Cai, G.; Fung, K.; Ng, K. Process Development for the Recycle of Spent Lithium Ion Batteries by Chemical Precipitation. *Ind. Eng. Chem. Res.* **2014**, *53*, 18245–18259. [CrossRef]
104. Geng, H.; Wang, F.; Yan, C.; Tian, Z.; Chen, H.; Zhou, B.; Yuan, R.; Yao, J. Leaching behavior of metals from iron tailings under varying pH and low- molecular-weight organic acids. *J. Hazard. Mater.* **2020**, *383*, 121136. [CrossRef]
105. Mahandra, H.; Ghahreman, A. A sustainable process for selective recovery of lithium as lithium phosphate from spent $LiFePO_4$ batteries. *Resour. Conserv. Recycl.* **2021**, *175*, 105883. [CrossRef]
106. Li, L.; Bian, Y.; Zhang, X.; Yao, Y.; Xue, Q.; Fan, E.; Wu, F.; Chen, R. A green and effective room-temperature recycling process of $LiFePO_4$ cathode materials for lithium-ion batteries. *Waste Manag.* **2019**, *85*, 437–444. [CrossRef] [PubMed]
107. Niu, Y.; Peng, X.; Li, J.; Zhang, Y.; Song, F.; Shi, D.; Li, L. Recovery of Li_2CO_3 and $FePO_4$ from spent LiFePO4 by coupling technics of isomorphic substitution leaching and solvent extraction. *Chin. J. Chem. Eng.* **2023**, *54*, 306–315. [CrossRef]
108. Dai, Y.; Xu, Z.; Hua, D.; Gu, H.; Wang, N. Theoretical-molar Fe3+ recovering lithium from spent LiFePO4 batteries: An acid-free, efficient, and selective process. *J. Hazard. Mater.* **2020**, *396*, 122707. [CrossRef]
109. Seo, E.; Cheong, Y.; Yim, G.; Min, K.; Geroni, J. Recovery of Fe, Al and Mn in acid coal mine drainage by sequential selective precipitation with control of pH. *Catena* **2017**, *148*, 11–16. [CrossRef]

110. Costa, M.; Pêczek, I.; Sadowski, Z.; Natu, S.; Paiva, P. The Solvent Extraction of Iron(III) from Chloride Solutions by N,N′-Tetrasubstituted Malonamides: Structure-Activity Relationships. *Solvent Extr. Ion Exch.* **2007**, *25*, 463–484. [CrossRef]
111. Muto, A.; Hirayama, Y.; Tokumoto, H.; Matsuoka, A.; Noishiki, K. Liquid–Liquid Extraction of Lithium Ions Using a Slug Flow Microreactor: Effect of Extraction Reagent and Microtube Material. *Solvent Extr. Ion Exch.* **2017**, *35*, 61–73. [CrossRef]
112. Masmoudi, A.; Zante, G.; Trébouet, D.; Barillon, R.; Boltoeva, M. Understanding the Mechanism of Lithium Ion Extraction Using Tributyl Phosphate in Room Temperature Ionic Liquid. *Solvent Extr. Ion Exch.* **2020**, *38*, 777–799. [CrossRef]
113. Wu, Y.; Zhou, K.; Zhang, X.; Peng, C.; Jiang, Y.; Chen, W. Aluminum separation by sulfuric acid leaching-solvent extraction from Al-bearing LiFePO4/C powder for recycling of Fe/P. *Waste Manag.* **2022**, *144*, 303–312. [CrossRef] [PubMed]
114. Wesselborg, T.; Virolainen, S.; Sainio, T. Recovery of lithium from leach solutions of battery waste using direct solvent extraction with TBP and $FeCl_3$. *Hydrometallurgy* **2021**, *202*, 105593. [CrossRef]
115. Costa, R.; Dugo, P.; Mondello, L. Chemistry, Molecular Sciences and Chemical Engineering. *Compr. Sampl. Sample Prep.* **2012**, *4*, 43–59.
116. Lee, P.; Li, C.; Chen, J.; Li, Y.; Chen, S. Dissolution of D_2EHPA in liquid–liquid extraction process: Implication on metal removal and organic content of the treated water. *Water Res.* **2011**, *45*, 5953–5958. [CrossRef] [PubMed]
117. Kocherginsky, N.M.; Yang, Q. Big Carrousel mechanism of copper removal from ammoniacal wastewater through supported liquid membrane. *Sep. Purif. Technol* **2007**, *54*, 104–116. [CrossRef]
118. Liu, Q.; Tang, X.; Wang, Y.; Yang, Y.; Zhang, W.; Zhao, Y.; Zhang, X. ROS changes are responsible for tributyl phosphate (TBP)-induced toxicity in the alga Phaeodactylum tricornutum. *Aquat. Toxicol.* **2019**, *208*, 168–178. [CrossRef]
119. MacCabe, W.; Smith, J.; Harriot, P. *Unit Operations of Chemical Engineering*, 5th ed.; McGraw-Hill: New York, NY, USA, 1993; pp. 623–632.
120. Geankoplis, C. *Transport Processes on Unit Operations*, 3rd ed.; Prentice-Hall: Minnesota, NJ, USA, 2003; pp. 697–743.
121. Torok, B.; Schafer, C.; Kokel, A. Solid catalysts for environmentally benign synthesis. In *Heterogeneous Catalysis in Sustainable Synthesis*; Elsevier: New Delhi, India, 2022; Volume 1, p. 229622.
122. Lebron, Y.; Moreira, V.; Amaral, M. Metallic ions recovery from membrane separation processes concentrate: A special look onto ion exchange resins. *Chem. Eng. J.* **2021**, *425*, 131812. [CrossRef]
123. Lv, R.; Hu, Y.; Jia, Z.; Li, R.; Zhang, X.; Liu, J.; Fan, C.; Feng, J.; Zhang, L.; Wang, Z. Removal of Fe3+ and Al3+ ions from phosphoric acid–nitric acid solutions with chelating resins. *Hydrometallurgy* **2019**, *188*, 194–200. [CrossRef]
124. Nasef, M.; Ujang, Z. Introduction to Ion Exchange Processes. In *Ion Exchange Technology I*; Springer: Dordrecht, Netherlands, 2012; Volume 1, pp. 1–39.
125. Virolainen, S.; Wesselborg, T.; Kaukinen, A.; Sainio, T. Removal of iron, aluminium, manganese and copper from leach solutions of lithium-ion battery waste using ion exchange. *Hydrometallurgy* **2021**, *202*, 105602. [CrossRef]
126. Zhang, X.; Liu, Z.; Qu, D. Proof-of-Concept study of ion-exchange method for the recycling of LiFePO4 cathode. *Waste Manag.* **2023**, *157*, 1–7. [CrossRef]
127. Becht, G.; Vaughey, J.; Britt, R.; Eagle, C.; Hwu, S. Ion exchange and electrochemical evaluation of the microporous phosphate $Li_9Fe_7(PO_4)_{10}$. *Mater. Res. Bull.* **2008**, *43*, 3389–3396. [CrossRef]
128. Hermassi, M.; Granados, M.; Valderrama, C.; Skoglund, N.; Ayora, C.; Cortina, J. Impact of functional group types in ion exchange resins on rare earth element recovery from treated acid mine waters. *J. Clean. Prod.* **2022**, *379*, 134742. [CrossRef]
129. Vinco, J.; Botelho Junior, A.; Duarte, H.; Espinosa, D.; Tenório, J. Purification of an iron contaminated vanadium solution through ion exchange resins. *Miner. Eng.* **2022**, *176*, 107337. [CrossRef]
130. Perez, I.; Correa, M.; Tenório, J.; Espinosa, D. Effect of the pH on the Recovery of Al^{3+}, Co^{2+}, Cr^{3+}, Cu^{2+}, Fe^{3+}, Mg^{2+}, Mn^{2+}, Ni^{2+} and Zn^{2+} by Purolite S950. Energy Technology. *Miner. Met. Mater. Ser.* **2018**, *2018*, 385–393.
131. Song, Y.; Zhao, Z. Recovery of lithium from spent lithium-ion batteries using precipitation and electrodialysis techniques. *Sep. Purif. Technol.* **2018**, *206*, 335–342. [CrossRef]
132. Li, Z.; He, L.; Zhu, Y.; Yang, C. A Green and Cost-Effective Method for Production of LiOH from Spent $LiFePO_4$. *Sustain. Chem. Eng.* **2020**, *8*, 15915–15926. [CrossRef]
133. Barrueto, Y.; Hernández, P.; Jiménez, Y.; Morales, J. Properties and application of ionic liquids in leaching base/precious metals from e-waste. A review. *Hydrometallurgy* **2022**, *212*, 105895. [CrossRef]
134. Wandt, J.; Lee, J.; Arrigan, D.; Silvester, D. A lithium iron phosphate reference electrode for ionic liquid electrolytes. *Electrochem. Commun.* **2018**, *93*, 148–151. [CrossRef]
135. Zhu, A.; Bian, X.; Han, W.; Cao, D.; Wen, Y.; Zhu, K.; Wang, S. The application of deep eutectic solvents in lithium-ion battery recycling: A comprehensive review. *Resour. Conserv. Recycl.* **2023**, *188*, 106690. [CrossRef]
136. Milevskii, N.; Zinov'era, I.; Zakhodyaeva, Y.; Voshkin, A. Separation of Li(I), Co(II), Ni(II), Mn(II), and Fe(III) from hydrochloric acid solution using a menthol-based hydrophobic deep eutectic solvent. *Hydrometallurgy* **2022**, *207*, 105777. [CrossRef]
137. Cabezas, R.; Zurob, E.; Gomez, B.; Merlet, G.; Plaza, A.; Araya-Lopez, C.; Romero, J.; Olea, F.; Quijada-Maldona, E.; Pino-Soto, L.; et al. Challenges and Possibilities of Deep Eutectic Solvent-Based Membranes. *Ind. Eng. Res.* **2022**, *61*, 17397–17422. [CrossRef]
138. Deep Eutectic Solvents: A Review of Fundamentals and Applications. U.S. Department of Energy. 2020. Available online: https://www.energy.gov/ (accessed on 1 February 2023).

139. Schiavi, P.; Altimari, P.; Branchi, M.; Zanoni, R.; Simonetti, G.; Navarra, M.; Pagnanelli, F. Selective recovery of cobalt from mixed lithium ion battery wastes using deep eutectic solvent. *Chem. Eng. J.* **2021**, *417*, 129249. [CrossRef]
140. Jing, Q.; Zhang, J.; Liu, Y.; Yang, C.; Ma, B.; Chen, Y.; Wang, C. E-pH Diagrams for the Li-Fe-P-H_2O System from 298 to 473 K: Thermodynamic Analysis and Application to the Wet Chemical Processes of the $LiFePO_4$ Cathode Material. *J. Phys. Chem.* **2019**, *123*, 14207–14215. [CrossRef]